THE IMPORTANCE OF THE ACYLTRANSFERASE LYCAT ON PI3K-AKT SIGNALING AND CANCER CELL PROLIFERATION

by

Victoria Chan

B.Sc. (Hons), Queen's University, 2019

A thesis presented to Ryerson University

in partial fulfillment of the

requirements for the degree of

Master of Science

in the program of

Molecular Science

Toronto, Ontario, Canada, 2022

AUTHOR'S DECLARATION FOR ELECTRONIC SUBMISSION OF A THESIS

I hereby declare that I am the sole author of this thesis. This is a true copy of the thesis, including any required final revisions, as accepted by my examiners.

I authorize Ryerson University to lend this thesis to other institutions or individuals for the purpose of scholarly research.

I further authorize Ryerson University to reproduce this thesis by photocopying or by other means, in total or in part, at the request of other institutions or individuals for the purpose of scholarly research.

I understand that my thesis may be made electronically available to the public.

THE IMPORTANCE OF THE ACYLTRANSFERASE LYCAT ON PI3K-AKT SIGNALING AND CANCER CELL PROLIFERATION

Victoria Chan

Master of Science, 2022

Molecular Science, Ryerson University

ABSTRACT

Phosphoinositides (PIPs) play a key role in regulating key cellular functions. PIPs are enriched with a unique acyl profile composed of stearate and arachidonate at the sn-1 and sn-2 positions, respectively, which is governed by phospholipase As and acyltransferases. Specifically, lysocardiolipin acyltransferase (LYCAT) incorporates stearic acid onto the sn-1 position. Previous work found that LYCAT silencing selectively perturbs the levels and localization of phosphatidylinositol-4,5-bisphosphate, an important precursor for phosphatidylinositol-3,4,5-trisphosphate (PIP_3). PIP_3 recruits and modulates the effector Akt, which promotes and coordinates cell survival and proliferation. Thus, we hypothesized that LYCAT is important in PIP_3-Akt signaling and cell proliferation. Our results show that LYCAT silencing suppresses EGF-stimulated phosphorylation of Akt and select downstream substrates. Further, we observed impaired cell proliferation. Overall, our results suggest that the acyl specificity governed by LYCAT may play a significant role in controlling cell signaling and proliferation, which may have consequences for diseases such as cancer.

ACKNOWLEDGEMENTS

Firstly, I would like to thank my supervisors Dr. Costin Antonescu and Dr. Roberto Botelho for giving me the opportunity to pursue an MSc in their labs. I could not have asked for better supervisors and mentors. I am extremely grateful for your unwavering support, advice, and words of encouragement, especially when experiments didn't go as planned. Thank you for challenging me and investing in my personal growth. It is evident that you both care deeply for your students, and I am lucky to have spent the last few years under your supervision. I would also like to extend my thanks to my supervisory committee, Dr. Michael Olson and Dr. Mathieu Lemaire. Thank you for your insight and guidance.

I want to thank my lab mates in the Antonescu and Botelho labs for always being willing to help and lend a hand. Thank you for making our labs a safe and fun environment. I want to thank Dr. Stephen Bautista, for being an incredibly patient teacher and mentor. I also want to thank Dr. Kai Zhang for being my go-to person when I needed help or a good laugh. I would also like to thank Ella Hyatt, for her effort in maintaining the spaces and equipment at our research facility in MaRS.

To my friends and family, thank you for being my greatest support system. To my parents, thank you for instilling in me the importance of hard work and perseverance, two things that got me through my graduate studies. Thank you for always believing in me and supporting me in all my endeavours. To my sister, Megan, thank you for being there for me every step of the way; I couldn't have done it without you.

TABLE OF CONTENTS

LIST OF FIGURES

LIST OF ABBREVIATIONS

4E-BP1	Eukaryotic translation initiation factor 4E binding protein 1
AGPAT	Acylglycerol-3-phosphate O-acyltransferase
CDP-DAG	Cytidine diphosphate diacylglycerol
CDS	CDP-DAG synthases
CME	Clathrin mediated endocytosis
DAG	Diacylglycerol
DGKε	Diacylglycerol kinase epsilon
EE	Early endosome
EGF	Epidermal growth factor
EGFR	Epidermal growth factor receptor
ER	Endoplasmic reticulum
ERK	Extracellular signal-regulated kinases
Gab1	Growth factor receptor protein 1
GAP	GTPase activating protein
GPCR	G protein coupled receptor
Grb2	Growth factor receptor-bound protein 2
GSK3ß	Glycogen synthase kinase 3ß
LPA	Lysophosphatidic acid
LYCAT	Lysocardiolipin acyltransferase
MAPK	Mitogen-activated protein kinases
MBOAT	Membrane bound O-acyltransferase

MDM2	Murine double minute 2
mTOR	Mammalian target of rapamycin
mTORC1	mTOR complex 1
mTORC2	mTOR complex 2
PA	Phosphatidic acid
PDK1	Phosphoinositide-dependent kinase-1
PH	Pleckstrin homology
PI	Phosphatidylinositol
PI(3,4,5)P_3	Phosphatidylinositol-3,4,5-trisphosphate
PI(3,4)P_2	Phosphatidylinostiol-3,4,-bisphosphate
PI(3,5)P_2	Phosphatidylinositol-3,5-bisphosphate
PI(3)P	Phosphatidylinositol-3-phosphate
PI(4,5)P_2	Phosphatidylinositol-4,5-bisphosphate
PI(4)P	Phosphatidylinositol-4-phosphate
PI(5)P	Phosphatidylinositol-5-phosphate
PI3K	Phosphatidylinositol 3-kinase
PI4K	Phosphatidylinositol 4-kinase
PIP	Phosphoinositide
PIP5K	PI(4)P 5-kinase
PIS	Phosphatidylinositol synthase
PKB	Protein kinase B
PLA1	Phospholipase A1

PLA2	Phospholipase A2
PLC	Phospholipase C
PM	Plasma membrane
PTEN	Phosphatase and tensin homolog
RTK	Receptor tyrosine kinase
S6K	Ribosomal protein S6 kinase beta-1
SHIP	src-homolohy 2-containing inositol 5-phosphatase
TSC2	Tuberous sclerosis complex 2

CHAPTER 1: INTRODUCTION

1.1 An introduction to phospholipids

1.1.1 The different types of membrane lipids

Lipids are water insoluble molecules that are highly soluble in organic solvents. They serve a variety of biological roles including membrane structure, energy and heat stores, signaling and molecular markers to help identify specific organelles (Yang & Han, 2016). Lipids are the main component of the cell membrane and are diverse in their structure, distribution and composition. The lipid molecules present in cell membranes are amphipathic, meaning they contain both a hydrophilic and hydrophobic end. The shape and amphipathic nature of these molecules cause them to form bilayers in aqueous environments. Lipid molecules spontaneously aggregate to bury their hydrophobic tail in the interior and expose their hydrophilic heads to water. The most abundant structural lipid present in both the outer plasma membrane (PM) and internal organelle membranes are glycerophospholipids. Glycerophospholipids are considered the major class of lipids and consist of a glycerol backbone with fatty acids attached to the *sn*-1 and *sn*-2 positions (Figure 1.1). The headgroup consists of a phosphate linked at the *sn*-3 position with an alcohol attached to the phosphate (Bozelli & Epand, 2019). The common alcohol moieties of glycerophospholipids are serine, ethanolamine, choline, glycerol and inositol, with the head group substituent conferring the name of the glycerophospholipid. In addition to head group diversity, the variety and different combinations of fatty acids lead to diversity among the different membrane lipids.

1.1.2 Fatty acid diversity of lipids

The fatty acid chains present in glycerophospholipids vary in chain length, degree of unsaturation, the position of double bonds and hydroxylation. Fatty acids are written as (X:Y, n-Z), where X refers to the number of carbons in the chain, Y indicates the number of double bonds present, and Z is the position of the first double bond from the carboxylic acid end. Palmitic acid (16:0), stearic acid (18:0) oleic acid (18:1, n-9), linoleic acid (18:2, n-6) and arachidonic acid (20:4, n-6) are examples of fatty acids that can be incorporated onto phospholipids (Figure 1.1). In glycerophospholipids, the fatty acid at the *sn*-1 position tends to be saturated or monounsaturated, while the fatty acid attached to the *sn*-2 position is either mono- or poly-unsaturated (Yabuuchi & O'Brien, 1968). The different combinations of fatty acids attached to glycerophospholipids generates chemical diversity among the membrane lipids, however, some glycerophospholipids have highly specific acyl chain profiles. The acyl chain profile of phosphatidylinositol (PI) is less diverse than other glycerophospholipids and is highly enriched with a stearoyl (18:0) chain at the *sn*-1 position and an arachidonoyl (20:4) chain at the *sn*-2 position (Hicks et al., 2006). The acyl chain specificity of PI will be further expanded on in section 1.3.2. The acyl chain composition of these lipids influences the physical properties of the membrane.

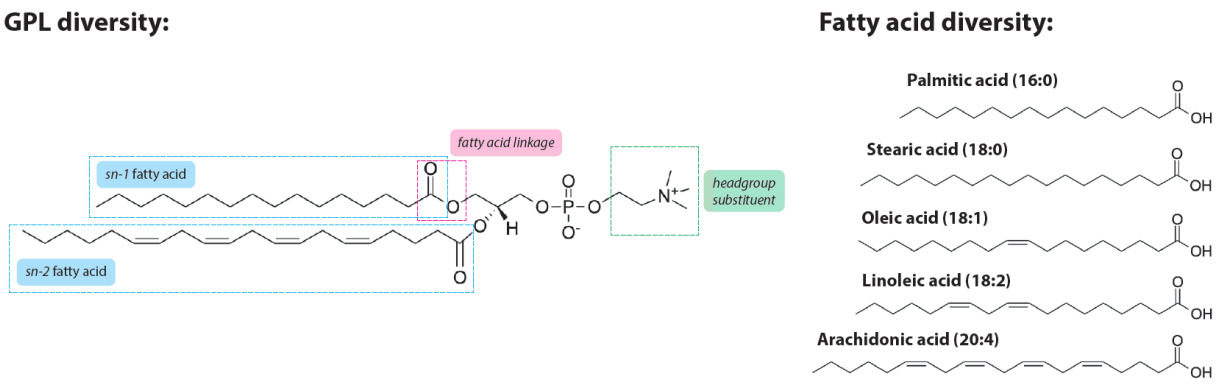

Figure 1.1: Membrane lipid and fatty acid diversity

Glycerophospholipids consist of a headgroup attached to a glycerol backbone with two fatty acyl chains attached to the *sn-1* and *sn-2* positions. Examples of different fatty acids and their structures are shown; X indicates the number of carbons and Y is the number of double bonds (X:Y).

1.2 An introduction to phosphoinositides (PIP)

1.2.1 PIP structure

As previously mentioned, PI is a member of the glycerophospholipid family, which are a family of major structural lipids present in eukaryotic membranes (Van Meer et al., 2008). The hydrophobic portion of PI contains saturated or *cis*-unsaturated fatty acyl chains of varying lengths at the *sn*-1 and *sn*-2 positions (Bozelli & Epand, 2019; Van Meer et al., 2008). The diacylglycerol (DAG) backbone connects the acyl chains to the inositol head group through the D1 phosphate group on the inositol ring (Figure 1.2). The inositol head group has free hydroxyl groups at positions D2 through to D6, and those at D3, D4 and D5 can be phosphorylated by several cytoplasmic lipid kinases (Falkenburger et al., 2010). Phosphorylation of PI generates seven possible PIPs consisting of a variety of monophosphorylated PIPs, (phosphatidylinositol 3-

phosphate (PI(3)P), phosphatidylinositol 4-phosphate (PI(4)P), phosphatidylinositol 4-phosphate (PI(5)P)), bis-phosphorylated species, (phosphatidylinositol 3,4-bisphosphate ($PI(3,4)P_{2)}$, phosphatidylinositol 3,5-bisphosphate ($PI(3,5)P_{2)}$, phosphatidylinositol 4,5-bisphosphate ($PI(4,5)P_2$)), and one tris-phosphorylated species, phosphatidylinositol 3,4,5-trisphosphate ($PI(3,4,5)P_3$). Each of these PIP species are found on different membranes and organelles.

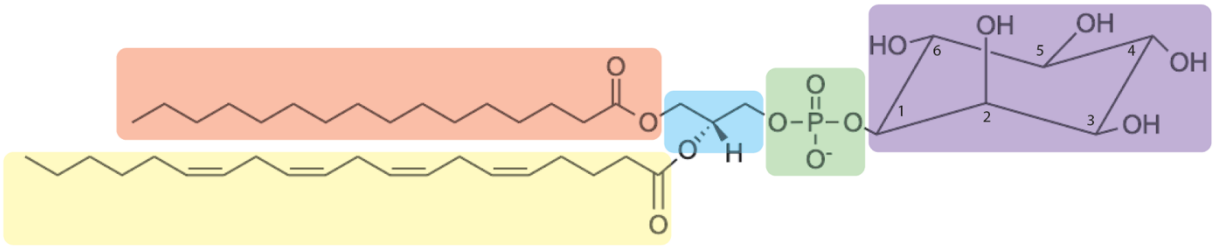

Figure 1.2: Phosphatidylinositol structure

The species presented is 1-stearoyl-2-arachidonoyl-*sn*-glycero-3-phospho-(1-*myo*-inositol). The stearic acid (18:0) is depicted in red and is located at the *sn*-1 position, while the arachidonic acid (20:4) is located at the *sn*-2 position, depicted in yellow. The acyl chain is connected to the glycerol backbone (blue), phosphate (green) and inositol head (purple). The inositol ring is numbered, indicating the different positions that it can be phosphorylated on.

1.2.2 PIP metabolizing and converting enzymes

The metabolizing enzymes that are responsible for the interconversion between PIP species are the PIP kinases and phosphatases. These specific metabolizing enzymes are able to generate seven different PIP species through the addition or removal of a phosphate group by kinases and phosphatases, respectively. For example, phosphatidylinositol 4-kinase (PI4K) phosphorylates PI to yield PI(4)P which can be further phosphorylated by PI(4)P 5-kinase (PIP5K) to generate

$PI(4,5)P_2$ (Sasaki et al., 2009). Class I phosphatidylinositol 3-kinase (PI3K) is responsible for converting $PI(4,5)P_2$ to $PI(3,4,5)P_3$ and PI(4)P to $PI(3,4)P_2$, while phosphatase and tensin homolog (PTEN) converts $PI(3,4,5)P_3$ back to $PI(4,5)P_2$. These enzymes will be further expanded upon in section 1.4.2. Figure 1.3 shows the kinase and phosphatases responsible for generating the seven different PIP species.

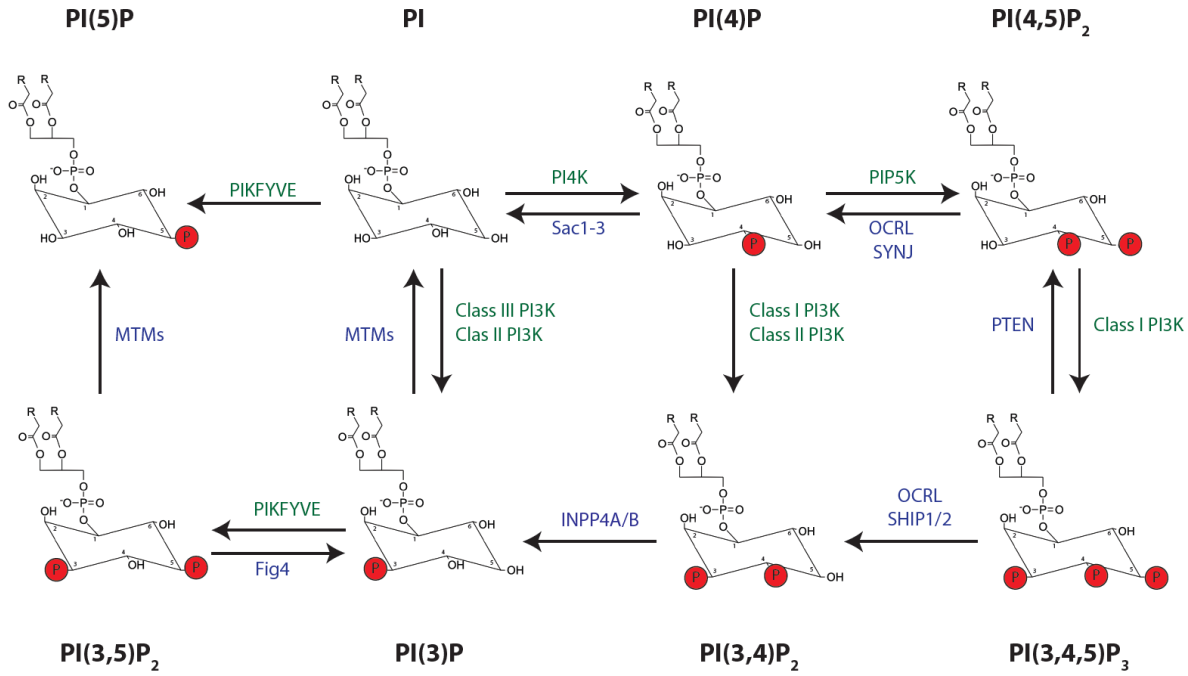

Figure 1.3: Interconversion of PIP species by kinases and phosphatases

PIP kinases are responsible for the addition of a phosphate group (red) onto the inositol headgroup, while phosphatases remove them. The interconversion between different PIP species is indicated by an arrow with its respective PIP metabolizing enzyme. Based on (Wallroth & Haucke, 2018)

1.2.3 PIP localization

The phospholipid composition of different membranes varies throughout the cell, allowing the cell to differentiate between compartments. The cell relies on specific membrane identities which is ultimately controlled by PIPs. PIPs were previously thought to be restricted to single organelles however, we are now realizing that PIP localization is quite complex. For example, PI(4)P, typically associated with the *trans*-Golgi and secretory vesicles, has also been shown to localize to the lysosome (Jeschke et al., 2015). PI(4,5)P_2 is a key lipid messenger that was previously described to be localized primarily at the PM, but has since been shown to localize to other intracellular compartments. Although a majority of PI(4,5)P_2 is found at the PM, studies have revealed that a substantial pool of PI(4,5)P_2 is localized to organelles such as endosomes, autophagosomes, and the nucleus (Hammond & Balla, 2015; Lemmon & Ferguson, 2000; Watt et al., 2002). PI(3,4,5)P_3 is mainly found on the PM but is also enriched in the nuclear envelope and in early endosomes (EE) (Jethwa et al., 2015). Figure 1.4 illustrates the complex and dynamic localization of PIP species.

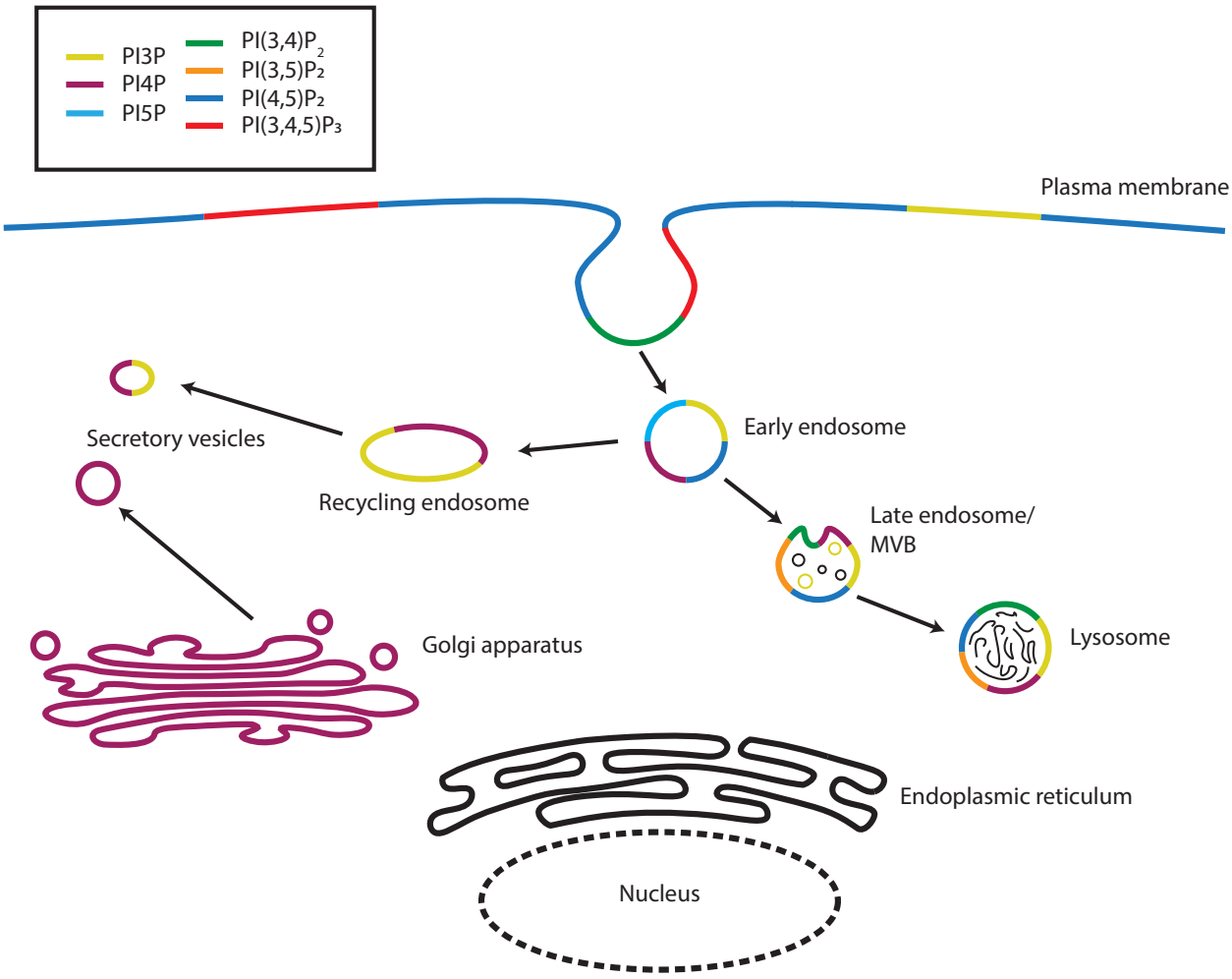

Figure 1.4: Cellular distribution of PIP species

PIP localization based on headgroup phosphorylation. Each PIP species is localized to distinct membranes within the cell, sometimes clustering on specific membranes. Some membranes are enriched with higher concentrations of certain species over others. Based on (Choy et al., 2017)

1.2.4 PIP function

While PIPs make up only 1-10% of total phospholipids, they control many aspects of a cell's functions (Balla, 2013). PIPs play an important role in regulating organelle dynamics, vesicular transport, signal transduction and membrane trafficking (Di Paolo & De Camilli, 2006; Mayinger, 2012). They have been shown to be involved in a number of signalling pathways that are essential

to maintaining cell physiology. Each PIP species is responsible for specific cellular functions. PI(4)P recruits proteins involved in Golgi trafficking to the Golgi membrane and promotes anterograde transport of secretory proteins from the Golgi to the PM (Audhya et al., 2000). PI(4,5)P_2 is a key lipid messenger at the PM that is also involved in regulating actin dynamics and endocytosis. PI(3,4,5)P_3 is involved in a number of cellular processes that control cell survival, proliferation and motility. Since PI(4,5)P_2 and PI(3,4,5)P_3 are a critical component of my thesis, they will be addressed in more detail in section 1.5.1. PIPs are able to perform their designated cellular functions through the recruitment of effector proteins.

1.2.5 PIP effector proteins

PIPs are able to perform their wide range of cellular activities through interactions with various effector proteins that contain PIP binding motifs (Cullen et al., 2001). PI(4,5)P_2 acts as a substrate for phospholipase C (PLC) following G protein coupled receptor (GPCR) activation and recruits adaptor proteins such as AP-2 and dynamin to the PM to regulate clathrin mediated endocytosis (CME) (Achiriloaie et al., 1999). Activation of PI3K phosphorylates PI(4,5)P_2 to produce PI(3,4,5)P_3 which recruits effector molecules that contain pleckstrin homology (PH) domains, such as Akt and phosphoinositde-dependent kinase-1 (PDK1) (Lien et al., 2017). Activation of these effector proteins regulate a variety of different cellular functions including cell survival, proliferation, metabolism and growth.

1.2.6 Acyl chain composition

Until recently, studies have focused on the importance of differentiation on the inositol headgroup. Research has only since begun investigating the importance of the specific acyl chain composition of these phospholipids. This is of importance because changes in acyl chain composition can affect PIP regulation and function, for example, membrane trafficking (Boneet al., 2017). Lipid kinases such as PIP5K and the 5-phosphatases, OCRL and synatpojanin-1, have shown specificity and higher enzyme kinetics for the C38:4 acyl chain profile of PI(4,5)P_2 (Schmid et al., 2004; Shulga et al., 2012). Enzyme kinetics, specifically substrate affinity (K_M) and catalytic turnover (V_{max}), revealed that the 5-phosphatases have sensitivity toward fatty acid composition (Schmid et al., 2004). Differences in acyl chain may also alter the way in which the polar inositol headgroup is presented for effector binding. PIP effectors interact with the inositol headgroup through their PIP-binding domains (Choy et al., 2017). Depending on the length and degree of unsaturation, the inositol headgroup may sit higher or lower in the membrane such that the effector cannot interact, or bind at all, with the membrane surface (Laux et al., 2000).

1.3 Incorporation of fatty acids onto PIPs

1.3.1 De novo synthesis of PIPs

The enrichment of specific acyl chain profiles on PIPs occurs via two pathways: *de novo* synthesis and the PIP remodelling pathway. The specificity of acyl chain profiles can arise from these two parallel pathways. The *de novo* synthesis of PI is thought to occur at the endoplasmic reticulum (ER). Synthesis begins with the acylation of two precursors, yielding lysophosphatidic acid (LPA) and phosphatidic acid (PA) (D'Souza & Epand, 2014). PA is then converted to cytidine

diphosphate diacylglycerol (CDP-DAG) through CDP-DAG synthases (CDS). Finally, PI synthase (PIS) couples CDP-DAG to *myo*-inositol to form PI (Figure 1.5). The *de novo* synthesis generates PI with mainly saturated and monounsaturated acyl chains (Hicks et al., 2006). The PI cycle also contributes to the synthesis of PI by feeding PA into the *de novo* pathway. PA is formed through the phosphorylation of DAG by the lipid kinase diacylglycerol kinase (DGK) (Figure 1.5).

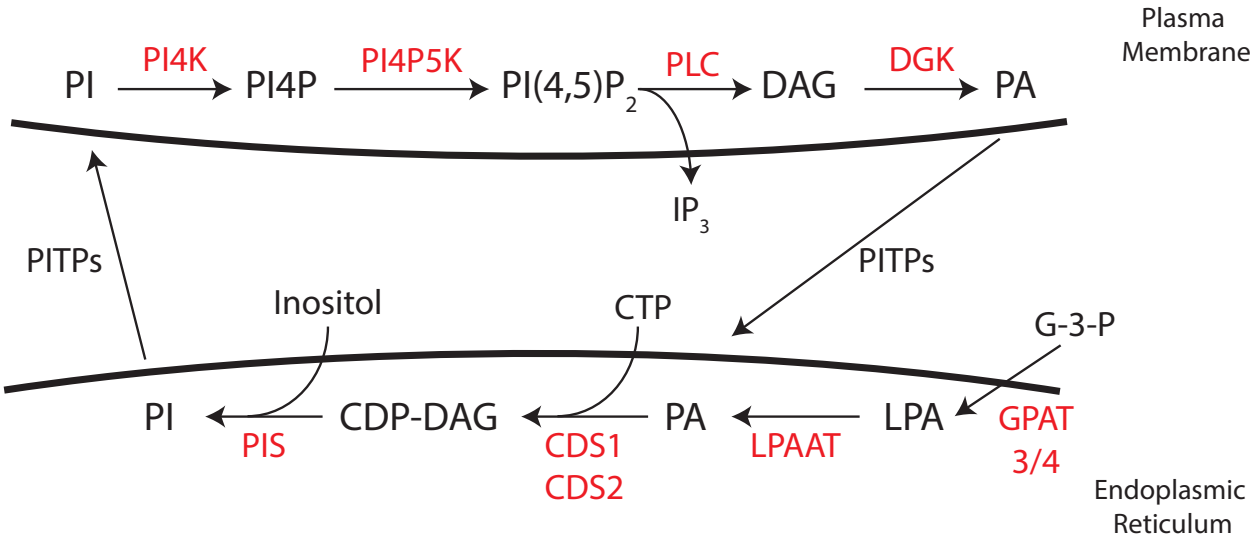

Figure 1.5: PI synthesis via the *de novo* synthesis pathway

De novo synthesis of PI occurs in the ER. The PI cycle, at the plasma membrane, contributes to PI synthesis by feeding phosphatidic acid into the *de novo* pathway.

1.3.2 Acyl chain remodelling of PI through the Lands' cycle

PI is highly enriched at the *sn*-1 and *sn*-2 positions with specific acyl chains. The most prominent species being 1-stearoyl-2-arachidnonyl PI, with a C38:4 fatty-acyl chain (18:0 *sn*-1/20:4 *sn*-2). Acyl chain remodelling allows lipids to maintain specific acyl chain compositions, which can be important for their unique functions. Incorporation of these selective acyl chain profiles is

through a process known as the Lands' cycle (D'Souza & Epand, 2014). The Lands' cycle relies on acyltransferases and phospholipases to enrich specific acyl chain profiles.

During the process of acyl chain remodelling, the fatty acyl groups attached to the glycerol backbone are removed and replaced with new acyl chains. Phospholipases and acyltransferases are responsible for deacylation and reacylation, respectively (Figure 1.6). Phospholipase A1 (PLA1) is a hydrolyzing enzyme that cleaves the fatty acid attached at the *sn*-1 position, producing a 2-acyl-lysophospholipid. Similarly, phospholipase A2 (PLA2) targets the *sn*-2 position of the glycerol moieties of phospholipids to generate a 1-acyl-lysophospholipid. Inhibition of PLA2 expression decreased levels of lysophosphatidylcholine and the ability of the cell to incorporate arachidonic acid onto the *sn*-2 position of membrane lipids (Balsinde et al., 1997). Phospholipase A1 (PLA1) activities have been detected in many cell and tissues types, however, only a limited number of PLA1s have been cloned and characterized thus far (Inoue & Aoki, 2017). Conversely, PLA2s are the most widely studied phospholipases. The PLA2 family is subdivided into several classes of enzymes that each have their own catalytic mechanism, localization, and structural and functional features (Aloulou et al., 2012). Once the fatty acid has been removed by phospholipases, lysophospholipid acyltransferases are responsible for reacylation of the lysophospholipid.

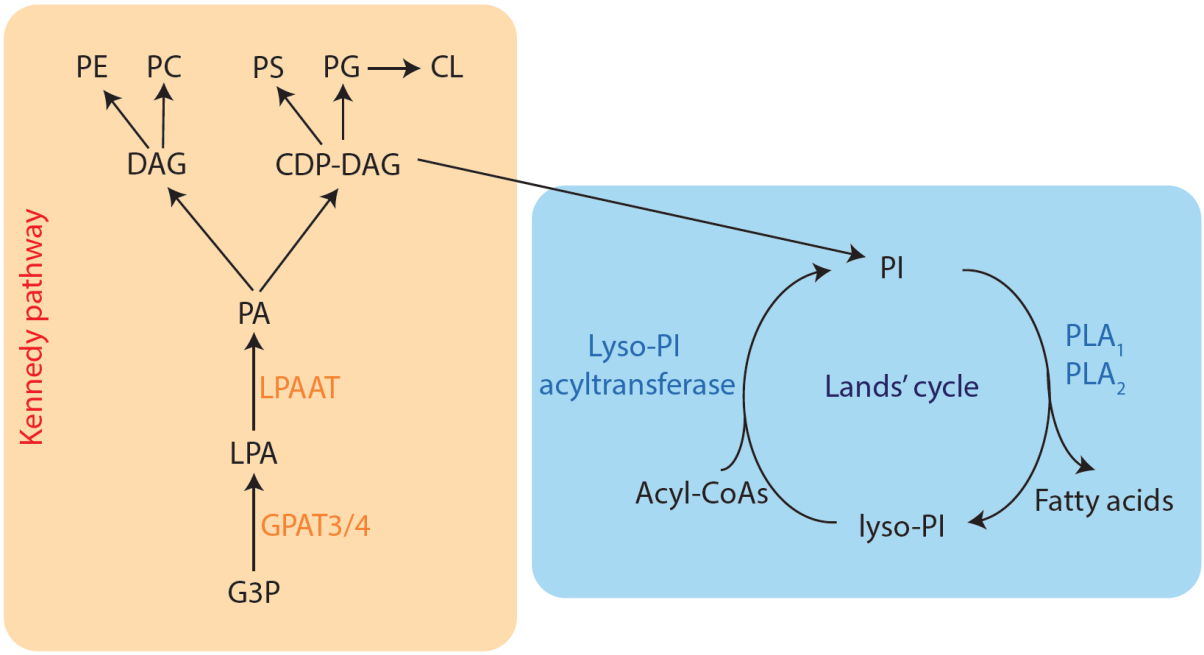

Figure 1.6: The Kennedy pathway and Lands' cycle

Phospholipid synthesis occurs via the Kennedy pathway, also referred to as the *de novo* pathway. Acyl chain remodelling occurs via the Land's cycle. In this pathway, phospholipase A1 and A2 (PLA_1 and PLA_2) are responsible for removing a fatty acid from PI. Lyso-PI acyltransferases reincorporate a fatty acid onto the lysophosphatidylinositol, resulting in a new acyl chain composition.

1.3.3 Acyltransferases involved in acyl chain remodelling of PI

Lysophospholipid acyltransferase have an important role to play in the Lands' cycle. They are responsible for incorporating fatty acyl chains back onto the lysophospholipids and require an acyl-coA ester as a substrate. These enzymes are classified into two families, the membrane bound O-acyltransferase (MBOAT) family and the 1-acylgylercol-3-phosphate acyltransferase (AGPAT) family. Both of these families have motifs that are essential for their lysophospholipid

acyltransferase activity (Shindou et al., 2009). Site directed mutagenesis revealed four MBOAT motifs and four AGPAT motifs (Shindou et al., 2009, 2017; Takeuchi & Reue, 2009). There are 4 known MBOAT isoforms, each with different acyl acceptors and products; MBOAT7 is known to have lysoPI activity and is responsible for incorporating arachidonate onto lysoPI (Shindou et al., 2009). Currently, 11 human AGPAT isoforms have been reported, each with different acyl acceptors and products. AGPAT1 and AGPAT2 remain the most well established AGPATs and possess acyltransferase activity towards lysoPA (Leung, 2001). The acyltransferase, lysocardiolipin acyltransferase (LYCAT), also named ALCAT1, AGPAT8 or LCLAT1, is another lysophospholipid acyltransferase that is postulated to be involved in acyl chain remodelling at the *sn*-1 position.

1.3.4 LYCAT expression and intracellular localization

LYCAT is a 414 amino acid membrane protein from the lysophospholipid acyltransferase family which have one conserved acyltransferase domain and three putative transmembrane domains. LYCAT has been shown to play critical roles in phospholipid metabolism through catalyzing the remodeling of CL, as well as several other phospholipids (Bone et al., 2017; J. Li et al., 2012; Zhao et al., 2009). LYCAT mRNA is widely expressed in various mouse tissues, but the highest expression was found in the heart and liver (Cao et al., 2004). Further, there is a shorter isoform of LYCAT mRNA found in specific tissues (Cao et al., 2004). Human LYCAT was found to be abundant in organs including heart, liver, lung, spleen and breast (Wang et al., 2010).

Initially, LYCAT was believed to localize to the ER, where most phospholipids' biosynthesis take place (Cao et al., 2004). An *in vitro* study analyzed subcellular fractions and found that LYCAT localized to the mitochondrial associated membrane which acts as membrane bridge connecting the ER and mitochondria (J. Li et al., 2010; Rieusset, 2018). Further, our group found that LYCAT is localized to ER-derived PIS-containing vesicles (Bone et al., 2017).

1.3.5 LYCAT function

LYCAT was first identified as an acyl-coA:lysocardiolipin acyltransferase involved in regulating the phospholipid, cardiolipin , found in the inner mitochondrial membrane (Cao et al., 2004). It was later shown that LYCAT$^{-/-}$ results in a reduction of stearate incorporation onto PI, but not of other phospholipids such as phosphatidylcholine, phosphatidylserine or phosphatidylethanolamine (Cao et al., 2004). Imae *et al* identified three *Caenorhabditis elegans* (*C. elegans*) acyltransferases, ACL-8, ACL-9 and ACL-10, that incorporate stearic acid onto the *sn*-1 position of PI; mammalian LYCAT is the closest homolog to these acyltransferases (Imae et al., 2012). Mutations in the genes that encode these acyltransferases cause a reduction in acyltransferase activity toward the *sn*-1 position. Additionally, in LYCAT$^{-/-}$ mice, there was a reduction of stearic acid at the *sn*-1 position of PI compared to wild-type mice (Imae et al., 2012).

In addition to remodeling PI, LYCAT has also been shown to alter the acyl chain profile of cardiolipin (Cao et al., 2004; Huang et al., 2014; Zhao et al., 2009). LYCAT plays a critical role in cardiolipin remodeling by catalyzing dilysocardiolipin to monolysocardiolipin and then back to cardiolipin (Cao et al., 2004, 2009). The mono- and di-lysocardiolipin recognition by LYCAT

depends on the fatty acyl-CoAs. Recombinant LYCAT expressed in Sf9 cells demonstrated predominant activity and selectivity toward linoleoyl-CoA and oleoyl-CoA, the two unsaturated C18 acyl chains (Cao et al., 2004).

In addition to its role in acyl chain remodeling, LYCAT is also involved in regulating the levels and localization of different PIP species. Work done by recent alumni of our lab, Dr. Leslie Bone, showed that LYCAT silencing reduces total levels of PI(3)P and PI(4,5)P_2 by 25% and 21%, respectively (Bone et al., 2017). Dr. Bone also found that LYCAT silencing alters the acyl chain profile of PIP_2 but not that of PI or PIP_1.

1.4. Receptor tyrosine kinase signaling

Receptor tyrosine kinases (RTK) are transmembrane cell surface receptor proteins that respond to specific extracellular growth factor ligands. These RTKs have roles to play in controlling cellular functions such as proliferation, growth and survival. In their inactive state, RTKs are monomeric but upon ligand binding, these receptors dimerize and trigger autophosphorylation and activation of the receptor (Du & Lovly, 2018).

1.4.1 EGFR signaling

Epidermal growth factor receptor (EGFR) is one of the most studied RTKs. Binding of the epidermal growth factor (EGF) ligand results in EGFR dimerization which leads to autophosphorylation of multiple tyrosine residues on the receptor's intracellular domain (Díaz et al., 2012). EGFR ligand binding leads to receptor internalization, ubiquitination and degradation.

EGFR is internalized via CME, whereby the receptor is removed from the cell surface via clathrin-coated pits (CCPs) (Sigismund et al., 2008) EGFR-ligand complexes are then trafficked to the EE, which then mature into sorting endosomes or multivesicular bodies. Receptors are either recycled to the cell surface or destined for degradation. The EE gradually loses its early endosome components (i.e. early endosomal antigen 1 (EEA1) and Rab5) and becomes enriched with late endosomal proteins, such as Rab7; thus, maturing into late endosomes. The endosomal sorting complexes required for transport (ESCRT) machinery sorts ubiquitinated EGFR onto the intraluminal vesicles of maturing endosomes (Tomas et al., 2014). Fusion of the late endosome with lysosomes leads to the degradation of EGFR.

1.4.2 Class I PI3K

PI3K is a lipid kinase that is activated by growth factors and takes part in the signal transduction events involved in cell growth and transformation (Soltoff et al., 1993). PI3K catalyzes the phosphorylation of PI on the D3 position of the inositol ring. There are three classes of PI3K, grouped based on lipid substrate specificity and sequence homology (Vanhaesebroeck et al., 1997). Since class I PI3K is the most studied and responsible for the direct conversion of $PI(4,5)P_2$ into $PI(3,4,5)P_3$, I will focus this discussion on class I PI3K.

Class I PI3K contains four isoforms of the catalytic subunit: p110α, p110ß, p110δ and p110γ. These isoforms are further grouped according to their regulatory subunits and connections to upstream signaling (Engelman et al., 2006)). Class IA PI3K encompasses three catalytic subunits (p110α, p110ß, p110δ) and five regulatory subunits (p85α, p85ß, p55α, p55γ and p50α) (Engelman et al., 2006)). Class I PI3Ks are activated by RTKs. Upon ligand binding, RTKs

are activated, resulting in the autophosphorylation of several tyrosine residues. The PI3K regulatory subunits form interactions with the phosphotyrosine residues. This leads to recruitment of p110 to the membrane leading to the activation of its catalytic activity(Burke & Williams, 2015; Hubbard & Miller, 2007). Active class I PI3K catalyzes the conversion of $PI(4,5)P_2$ to $PI(3,4,5)P_3$.

1.5 The PI3K-Akt Pathway

1.5.1 $PI(4,5)P_2$ and $PI(3,4,5)P3$

$PI(4,5)P_2$ and $PI(3,4,5)P_3$ are involved in regulating key cellular events that maintain homeostasis. Here, I will discuss the role that $PI(4,5)P_2$ and $PI(3,4,5)P_3$ play in PI3K-Akt signaling. $PI(4,5)P_2$ is localized mainly to the PM, where it interacts with many proteins to control certain cellular functions. $PI(4,5)P_2$ is the most abundant phosphoinositide in mammalian cells and represents >99% of PIP_2 on the PM (Mücksch et al., 2019). $PI(4,5)P_2$ is an important substrate for key enzymes such as PLC, PI3K, and 5-phosphatases, OCRL and synaptojanin 1 and 2. Through the action of class I PI3K, $PI(4,5)P_2$ acts as an important precursor lipid for $PI(3,4,5)P_3$ production.

$PI(3,4,5)P_3$ is important for Akt signaling and is responsible for activating a wide range of proteins through its interaction with their specific binding domains. $PI(3,4,5)P_3$ represents only a small percentage of total PIPs and is almost undetectable in resting cells; however, by the activation of class I PI3Ks, $PI(3,4,5)P_3$ levels rapidly increase in the inner leaflet of the PM (Milne et al., 2005). $PI(3,4,5)P_3$ interacts with its effectors through direct binding of its inositol head group to the PH domain of the protein (Rosen et al., 2012). Among its effectors is the

serine/threonine kinases Akt (also referred to as protein kinase B (PKB), one of the most well-known effectors of PI(3,4,5)P_3. Signal termination of PI3K-Akt signalling is primarily achieved by PTEN and src-homology 2-containing inositol 5-phosphatase (SHIP2), which dephosphorylates PI(3,4,5)P_3. The initial production of PI(3,4,5)P_3 by PI3K is observed within seconds to minutes of growth factor stimulation, followed by downregulation with timing that depends on the cell type and stimulus (Auger et al., 1989).

1.5.2 Akt signaling axis

Akt is a critical node in cell signaling downstream of growth factors, cytokines and other stimuli (Manning & Cantley, 2007). Akt exists as three isoforms, Akt1, Akt2 and Akt3, each with a N-terminal PH domain that allows them to bind to either PI(3,4)P_2 or PI(3,4,5)P_3 (Figure 1.7). More specifically, quantitative lipid imaging revealed that Akt1 and Akt3 preferentially bind PI(3,4,5)P_3 while the Akt2 isoform binds PI(3,4)P_2 (Figure 1.8) (Liu et al., 2018). All three isoforms of Akt follow the same activation mechanism and share some overlapping substrates, however, Akt isoforms have specific roles in signal transduction. This may, in part, be due to their unique localization and access to specific substrates. Akt1 and Akt3 are localized to the PM, as PI(3,4,5)P_3 production occurs mainly at this site. Akt2, in addition to being localized at the PM, is also localized and activated at endosomal sites (Liu et al., 2018).

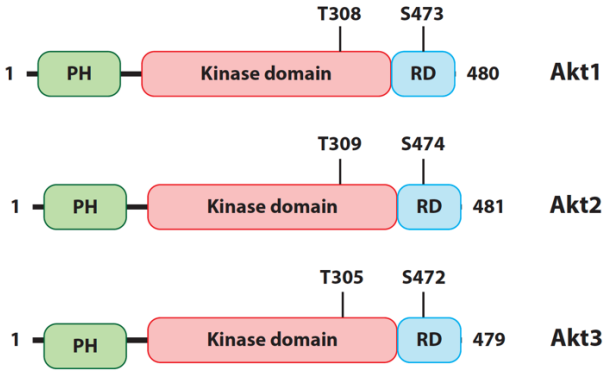

Figure 1.7: Comparison of Akt isoform domain structures

The Akt domain organization of the three Akt isoforms are mapped. All isoforms possess an N-terminal PH domain (green) responsible for phospholipid binding, a kinase or catalytic domain (red) which is critical for activation of the enzyme, and a regulatory domain (blue). Based on (Matheny & Adamo, 2009).

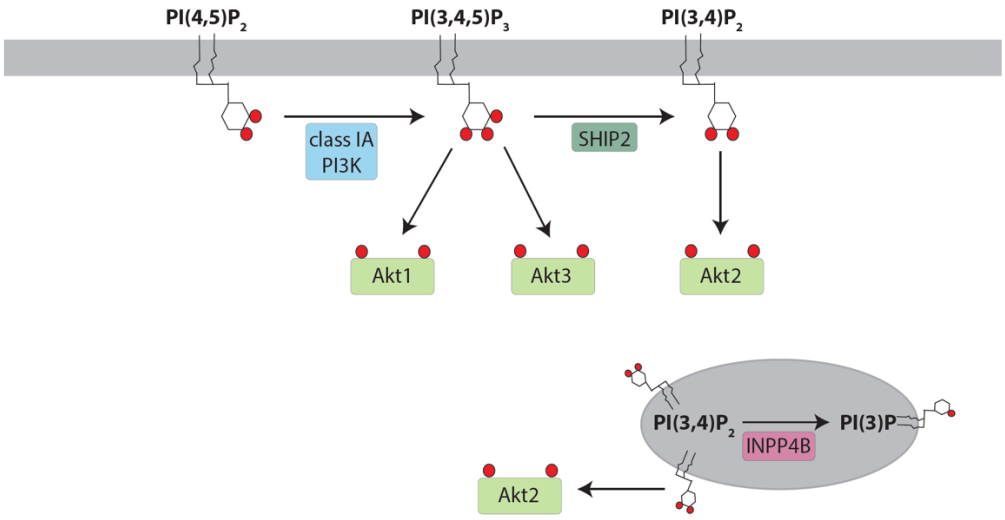

Figure 1.8: Akt isoforms bind specific PIPs

$PI(4,5)P_2$ is converted to $PI(3,4,5)P_3$ by class IA PI3K while SHIP2 dephosphorylates $PI(3,4,5)P_3$. Three isoforms of Akt exist, each preferentially binding to specific PIP species. Akt1 and Akt3 bind $PI(3,4,5)P_3$ while Akt2 binds $PI(3,4)P_2$.

1.5.3 PI3K-Akt signaling

The PI3K-Akt signalling axis controls cell survival, proliferation, metabolism, growth and is implicated in a variety of different cancers. The PI3K-Akt pathway is highly conserved and its activation involves a number of tightly controlled steps (Hemmings & Restuccia, 2012). Binding of the EGF ligand to EGFR results in receptor dimerization which ultimately leads to autophosphorylation of multiple tyrosine residues on the EGFR's intracellular domain (Díaz et al., 2012). The phosphorylation of these tyrosine residues recruits the adaptor proteins, growth factor receptor-bound protein 2 (Grb2) and growth factor receptor protein 1 (Gab1) via their proline rich domains. Src-mediated phosphorylation of Gab1 allows for binding of the p85 regulatory subunit of class IA PI3K (Díaz et al., 2012). The activation of class 1A PI3Ks allows for the conversion of $PI(4,5)P_2$ to $PI(3,4,5)P_3$. After this conversion, Akt binds to PIP_3 at the PM allowing PDK1 to phosphorylate the T308 residue of Akt. Phosphorylation at T308 results in only partial activation; mammalian target of rapamycin (mTOR) complex 2 (mTORC2) is required to phosphorylate Akt at the S473 residue. Phosphorylation at both sites stimulates its full activity. Full activation leads to additional substrate specific phosphorylation events in both the cytoplasm and nucleus (Figure 1.9).

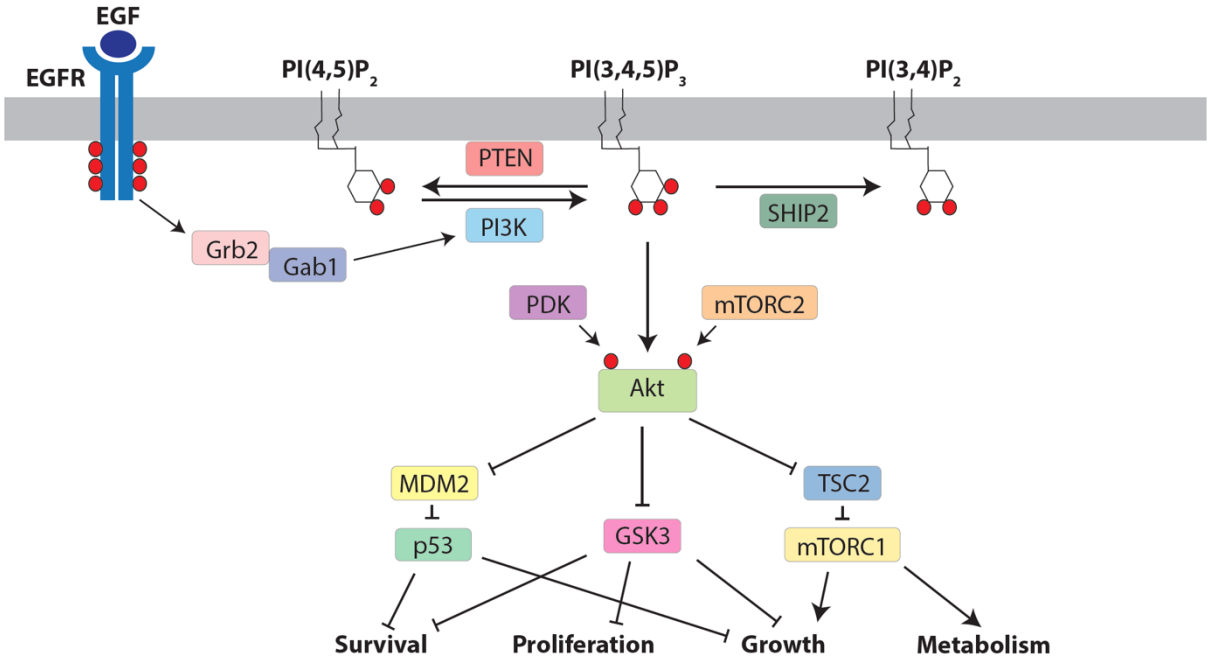

Figure 1.9: Substrates and Cellular Functions of the PI3K-Akt Pathway

Upon activation of EGFR, adaptor proteins are recruited to aid in the recruitment and activation of PI3K, converting $PI(4,5)P_2$ to PIP_3. This conversion activates Akt through phosphorylation at two sites, allowing for further Akt-mediated phosphorylation on many downstream substrates. These substrates are responsible for regulating a number of cellular functions.

1.5.4 Akt effectors

Akt regulates many downstream effectors that each have different roles to play in important cellular functions. The growth factor-regulated PI3K-Akt pathway has diverse downstream effects which regulate anabolic metabolism and cell growth. The PI3K-Akt pathway is involved in eukaryotic cell growth and metabolism through the Akt-mediated phosphorylation of key downstream effectors, namely mTOR complex 1 (mTORC1), glycogen synthase kinase 3ß (GSK3ß) and murine double minute 2 (MDM2) (Figure 1.9). mTORC1 is responsible for promoting the processes underlying cell growth such as protein, lipid and nucleotide synthesis as well as

inhibiting autophagy (Saxton & Sabatini, 2017). The primary mechanism by which Akt activates mTORC1 is through the phosphorylation and resulting inhibition of tuberous sclerosis complex 2 (TSC2). TSC2 acts as a GTPase activating protein (GAP) for Rheb GTPases, promoting the conversion of Rheb-GTP to Rheb-GDP. In its GTP-bound form, Rheb is involved in the activation of mTORC1; therefore, TSC2 acts as an inhibitor to mTORC1 (Manning & Toker, 2017). The Akt-mediated phosphorylation of TSC2 relieves the inhibitory effects on mTORC1 allowing it to become activated. Additionally, GSK3ß plays a key role in cellular metabolic reprogramming. GSK3ß is a multifunctional serine/threonine protein kinase which phosphorylates numerous downstream targets, such as members of the cyclin family, which are involved in cell cycle progression, as well as the proto-oncogenes, c-*jun* and c-*myc* which promote the transcription of survival and growth genes (Manning & Toker, 2017). GSK3ß-mediated phosphorylation often labels these targets for proteasomal degradation (Duda et al., 2020). Akt exerts an inhibitory phosphorylation on GSK3ß, preventing the degradation and enhancing the stability of the previously mentioned proteins, promoting proliferation. Further, the PI3K-Akt pathway is able to regulate cell growth, in part, through MDM2. MDM2 is an oncoprotein that promotes cell survival and cell cycle progression by inhibiting the p53 tumour suppressor protein. In order to regulate p53, MDM2 must gain nuclear entry. Akt-mediated phosphorylation of MDM2 results in its translocation from the cytoplasm into the nucleus. Nuclear entry of MDM2 diminishes cellular levels of p53 (Abraham & O'Neill, 2014). Dysregulation of this pathway can lead to a number of pathological disease states.

1.5.5 Dysregulation of PI3K-Akt and disease

Since the PI3K-Akt pathway plays a critical role in regulating diverse cellular functions such as metabolism, growth and survival, its dysregulation often leads to a number of human diseases. The dysregulation of Akt substrates may lead to diseases such as diabetes, cardiovascular disease, and cancer. Briefly, Akt2 knockout mice were diabetic and were impaired in their ability of insulin to lower blood glucose levels (Cho et al., 2001). In relation to cardiovascular disease, it was found that long term Akt1 activation results in hypertrophy with pathological attributes such as contractile dysfunction (Shiojima et al., 2005). The PI3K-Akt pathway has been found to be dysregulated in almost all human cancers. While a number of mutations in this pathway can exist in cancer, some of the more common mutations include overexpression of RTKs, elevated PI3K activity, and loss of PTEN (Hers et al., 2011).

OBJECTIVES AND RATIONALE

Previous research has focused on the phosphorylation of the inositol head group of PIPs; however, current studies are beginning to highlight the importance of the acyl chain composition. LYCAT has been shown to preferentially incorporate specific acyl chain profiles. However, the role of LYCAT in controlling PIP acyl chain species and the functional consequences that come with these unique acyl chain profiles remains unknown. Previous work done by Dr. Leslie Bone, a former PhD of our labs, found that LYCAT silencing leads to a partial reduction in EGF-stimulated Akt phosphorylation and endomembrane traffic (Bone et al., 2017). However, since Akt phosphorylation of specific substrates requires Akt activity on specific membrane compartments, it is not known if and how LYCAT silencing may specifically or preferentially impact phosphorylation of specific Akt substrates. Additionally, since LYCAT silencing altered endocytosis and endosomal trafficking of the transferrin receptor, we also wanted to test whether LYCAT disruption would affect EGFR signaling.

I hypothesize that LYCAT regulation of PIPs is essential for both Akt activation and localization on various membrane compartments, and as such selectively impacts specific Akt substrates. In addition, I hypothesize that LYCAT's ability to regulate Akt signaling will have a role to play in regulating cell growth. To test this hypothesis, I set the following project goals:

1. Determine the role of LYCAT on Akt signaling
2. Determine the role of LYCAT on EGFR dynamics
3. Determine the role of LYCAT on protein synthesis and cell proliferation

CHAPTER 2: MATERIALS AND METHODS

2.1 Cell culture

Wild-type ARPE-19 cells (CRL-2302 from ATCC), a retinal pigment epithelial cell line derived from the tissue of a 19-year-old male, were cultured in DMEM/F12 media obtained from ThermoFisher Scientific. MDA-MB-231 cells (HTB-26 from ATCC), breast epithelial cells isolated from a 51-year-old, White, female adenocarcinoma patient, were cultured in DMEM media (Wisent). MDA-MB-231 Cas9 tet-gLCLAT1 cells (see below for generation), were cultured in DMEM media obtained from Wisent. Both DMEM/F12 and DMEM were supplemented with 10% fetal bovine serum, 100 U/mL penicillin and 100 µg/mL streptomycin. Supplements were obtained from ThermoFisher Scientific and cells were cultured at 37°C and 5% CO_2.

2.2 Gene silencing by siRNA

To silence gene expression of LYCAT in both RPE-WT and MDA-MB-231 cells, custom-synthesized siRNA oligonucleotides against LYCAT were obtained, siLYCAT[1] with the sequence 5'-GGAAAUGGAAGGAUGACAAUU-3' and siLYCAT[2] with the sequence 5'-UCGAAGACAUGAUUGAUUAUU-3'. Additionally, a non-targeting control siRNA (NT siRNA) with the sequence 5'-CGUACUGCUUGCGAUACGGUU-3' was used. All oligonucleotides were obtained from Dharmacon. siRNA transfection was performed once cells reached 30-50% confluence using Lipofectamine RNAiMAX as per the manufacturer's instructions. For one well of a 6-well plate, 110 pmol of siRNA oligonucleotide (5.5 µL of 20 µM siRNA stock), 6.25 µL Lipofectamine RNAiMAX, and 100 µL of Opti-MEM medium were pre-complexed for 10 min at room temperature. During this time, cells were washed three times with phosphate buffered saline

(PBS) removing all traces of serum. Afterwards, the 100 µL siRNA pre-complex solution was added dropwise to cells in 900 µL Opti-MEM reduced-serum medium and incubated for 3 h. Following incubation, cells were washed once with PBS and replaced with 2 mL of regular growth media. Two rounds of transfection were performed, 24 h and 48 h after seeding; experimental assays were performed 72 h after seeding.

2.3 Gene silencing by an inducible CRISPR Cas9 system

MDA-MB-231 Cas9 tet-gLCLAT1 cells were obtained from the Salmena Lab at the University of Toronto. The following protocol was provided to us by Dr. Leonardo Salmena. Constitutive Cas9-expressing MDA-MB-231 cells were generated by infection with lenti Cas9-blast (Addgene: #52962). Generation of lentivirus was conducted using Calcium/phosphate transfections. HEK293T cells were seeded at a density of $1.5x10^6$ cells in a 10-cm dish 24 h prior to transfection and transfected as follows. Media was replaced 4 hours prior to transfection. For each 10 cm dish, 6.4 µg of psPAX2 (Addgene: #12260), 3.6 µg of pMD2.G (Addgene: #12259), 36 µL of 2 M $CaCl_2$ were mixed with 10 µg of lenti Cas9-blast (Addgene: #52962) into a final volume of 300 µL. 2X Hepes Buffered Saline (HBS; Sigma-Aldrich: 51558) was then added dropwise while vortexing. 48 hours after transfection, media was collected and lentiviral particles were concentrated by ultracentrifugation at 90,000 g for 90 min. Viral pellets were resuspended in DMEM and used directly or stored at -80 °C. $1x10^5$ MDA-MB-231 were seeded in 6 well dishes, the next day they were infected with 2 µL of concentrated virus + 2 µg/mL protamine sulfate in 2 mL of DMEM. After 2 days cells were expanded onto 10 cm dishes and cells were selected with 10 µg/mL

blasticidin for 7 days. After recovery, cells were initially screened for Cas9 activity through the GFP ablation assay.

Inducible *LCLAT* knockout MDA-MB-231 cells were generated by infecting Cas9+ MDA-MB-231 with pEZ-TET-pLKO-guide-puro which express the following gRNA sequences specific for *LYCAT. LCLAT* and control LacZ gRNA sequences were cloned as follows. pEZ-TET-pLKO-hygro was digested with EcoRI (NEB, R3101S) and NheI (NEB, R3131S) at 37°C, dephosphorylated with Antarctic Phosphate (NEB, M0289) for 1 hr at 37°C, and gel purified using the QIAquick Gel Extraction Kit (Qiagen, 28704). Three unique LCLAT guide RNAs were generated by PCR with AccuPrime Pfx Supermix (Invitrogen, 12344040). Lentiguide-Puro plasmid was used as the PCR template with the following primers: LacZ target forward (gctagcCCCGAATCTCTATCGTGCGGgttttagagctagaaatagcaagt) gLCLAT1-1 target forward (GGCCgctagcACAACCGCCTTGTGGCAACAgttttagagctagaaatagcaagt), gLCLAT1-2 target forward (GGCCgctagcTCTGATTGAGGAATGTTGTGgttttagagctagaaatagcaagt) and gLCLAT1-3 target forward (GGCCgctagcTGTAAAAGTGATTATAACTGgttttagagctagaaatagcaagt), universal scaffold reverse (CCGAATTCtcaagatctagttacgccaagctt). PCR products of 108bp were digested with EcoRI and NheI at 37°C O/N, and ligated into digested pEZ-tet-pLKO-hygro using T4 DNA Ligase (NEB, M0202) following the manufacturer's instructions. Ligation products were transformed into DH5α cells, maxiprepped with the QIAGEN Plasmid Maxi Kit (Qiagen, 12163) and verified by Sanger Sequencing.

Once generated, knockdown of LYCAT was achieved through 0.1 µg/mL or 1 µg/mL doxycycline induction for 5 days.

2.4 SDS-PAGE and Western blotting

Before lysate preparation, cells were serum starved for 1 h. Following siRNA transfection, cells were washed three times with PBS and incubated with 2 mL of serum free growth medium. After serum starvation, cells were stimulated with 5 ng/mL EGF for 5 and 10 min or left unstimulated (basal).

Following serum starvation and subsequent EGF stimulation, cells were washed 3 times in ice-cold PBS. Whole cell lysates were prepared in 200 µL 2X Laemmli Sample Buffer (0.5M Tris, pH 6.8, glycerol and 10% sodium dodecyl sulfate (SDS)) supplemented with protease and phosphatase inhibitors (1 mM sodium orthovanadate, 10 nM okadaic acid, 20 nM protease inhibitor cocktail). Lysates were heated at 65°C for 15 min and passed through a 27-gauge needle 10 times. Finally, 10% ß-mercaptoethanol and 5% bromophenol blue was added to cell lysates. Proteins were resolved by Tris-glycine SDS-PAGE; 4-20% mini-PROTEAN TGX precast polyacrylamide gel (BioRad), 1X SDS-PAGE running buffer (100 mL 10X Tris-glycine buffer, 10 mL 10% SDS, 890 mL ddH_2O) run at room temperature for 90 min (voltage starts at 120 V and is increased to 140 V once samples reach resolving gel). Following this, contents are transferred on to a polyvinylidene difluoride (PVDF) membrane through Western blotting at 100 V for 2 h at room temperature, on ice. The PVDF membrane was blocked for 1 h at room temperature in blocking buffer composed of 3% bovine serum albumin (BSA) in 1X final immunoblot wash buffer

(100 mL 10X base immunoblot, 0.5 mL Tween 20, 0.5 mL NP-40 alternative). After blocking, membranes were washed 3 times with wash buffer and incubated with 1:1000 primary antibody overnight at 4°C. The next day, membranes were washed 3 times, for 5 min each, and then subjected to 1:1000 secondary antibody for 1 h at room temperature. After incubation with secondary antibody, membranes were washed 3 times, for 5 min each, and imaged using the ChemiDoc imaging system by BioRad. Membranes were exposed to Immobilon Crescendo Western HRP substrate (Millipore Sigma) for 30-60 s and chemiluminescent images were acquired by the ChemiDoc. Western blot signals were analyzed and quantified using the ImageLab 6.1 program (BioRad). Band intensity was obtained by signal integration in an area corresponding to the appropriate land and band. This value was then normalized to the loading control signal. Phosphorylated protein levels were normalized to loading control and subsequently normalized to total protein levels relative to loading control.

Primary antibodies used were as follows: antibodies raised in rabbit were anti-LYCAT (cat. 106759) from GeneTex, anti-phospho-Akt (S473, cat. 9271), anti-phospho-Akt1 (S473, cat. 9018), anti-phospho-Akt2 (S474, cat. 8599), anti-Akt1 (cat. 2938), anti-phospho-EGFR (Y1068. Cat. 2234), anti-phospho-tuberin/TSC2 (T1462, cat. 3611), anti-tuberin/TSC2 (cat. 3612), anti-phospho-MDM2 (S166, cat. 3521), anti-MDM2 (cat. 86934), anti-phospho-GSK3ß (S9, cat. 9323), anti-clathrin (cat. 4796), and anti-GAPDH (cat. 2118) from Cell Signaling Technology. Antibodies raised in mouse were anti-Akt (cat. 2920), anti-Akt2 (cat. 5239), anti-GSK3ß (cat. 9832) and, anti-puromycin (cat. MABE343) from Cell Signaling Technology. Anti-EGFR (cat. 03-G) was raised in

goat and from Santa Cruz Biotechnology. Secondary anti-rabbit, anti-mouse and, anti-goat IgG horseradish peroxidase (HRP)-linked antibodies were from Cell Signaling Technology.

2.5 EGFR degradation assay

After 72 h of transfection, MDA-MB-231 cells were serum starved for 1 h followed by EGF stimulation (100 ng/mL) for 0, 30, 60, or 90 min. After serum stimulation, whole cell lysates were prepared and subjected to Western blot analysis as previously described; total EGFR levels were measured.

2.6 Puromycin incorporation assay

Following siRNA transfection, cells were treated with or without puromycin (10 µg/mL) for 10 min. Non-transfected control cells were treated with 10 µM cycloheximide for 20 min to block mRNA translation. Both puromycin and cycloheximide were obtained from Millipore Sigma. Whole cell lysates were prepared and subjected to Western blot analysis to probe for puromycin levels.

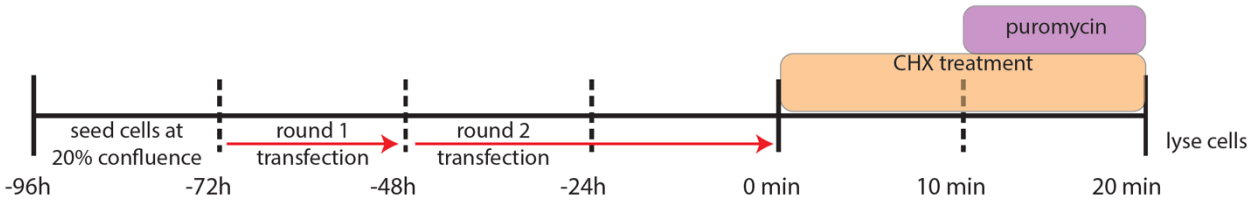

Figure 2.1: Puromycylation incorporation assay design

Cells were seeded at 20% confluence 96 h before t=0. After 72 h of transfection, CHX was added to non-transfected cells for 20 min, and puromycin to specific conditions for 10 min. After treatment, cells were lysed.

2.7 Incucyte live cell imaging

Cellular viability and cytotoxicity were measured using an Incucyte SX5 Live-Cell Analysis System (Sartorius). Cell death was assessed using 1 µL of CellTox Green Cytotoxicity Assay reagent (Promega G8741) diluted in 12 mL of DMEM. This mixture was added to cells prior to imaging. Images were acquired at 30-min intervals for 72 h under 10x magnification using brightfield phase contrast and 300 ms exposure of 460 nm excitation, 524 nm emission for green fluorescence.

For experiments using the CRISPR knockout cell line, cells were incubated with 1 µg/mL doxycycline for 3 days. On the third day, cells were reseeded for the experiment. The next day, CellTox Green dye was added to the media and imaging under the same conditions explained above occurred.

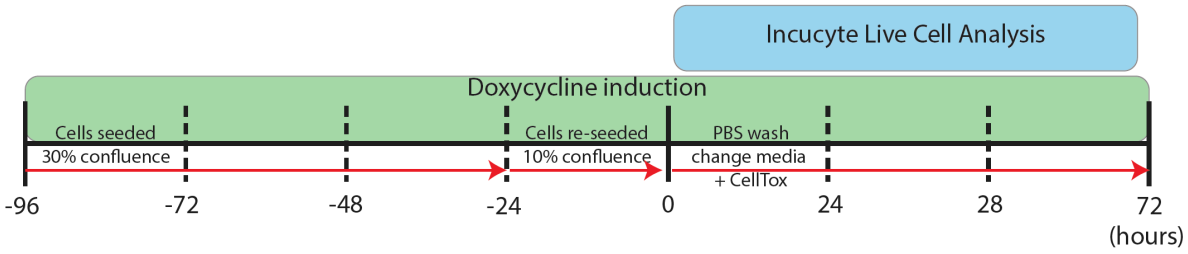

Figure 2.2: Incucyte proliferation and viability assay design for CRISPR cells

Cells were seeded at 30% confluence, 96 h before the experiment, then re-seeded on a 6-well plate at 10% confluence, 24 h prior to the experiment. On day 0, cells were washed with PBS and new media was added to cells. CellTox green dye was added to the media and images were acquired every 30 min for 72 h.

2.8 Statistical analysis

Experiments comparing two experimental conditions (i.e. NT siRNA and siLYCAT), were analyzed for statistical significance using an unpaired Student's *t* test with a two-tailed P value. Significant

pairwise comparisons were marked with asterisks on the graph, with $p < 0.05$ as a threshold for statistically significant differences between conditions. For experiments with two or more independent variables, a two-way ANOVA was conducted with Prism selecting Tukey's multiple comparison test. Significant pairwise comparisons were marked with asterisks on the graphs, with $p < 0.05$ as a threshold for statistically significant differences between conditions. All data are displayed as mean ± SEM and tests were conducted under the assumption of normality and sphericity. At least three independent experiments were conducted for all assays.

CHAPTER 3: RESULTS

3.1 Gene silencing methods target short and long isoform of LYCAT

3.1.1 LYCAT silencing using siRNA

To characterize the function of LYCAT in MDA-MB-231 cells, a triple negative breast cancer cell line, I used siRNA to knockdown LYCAT mRNA and thus, protein levels. To minimize the potential that observed phenotypes were due to off target effects, we designed two different oligonucleotides that targeted different sequences of LYCAT mRNA. Cells were transiently transfected with a non-targeting sequence (NT siRNA) or the oligonucleotides against LYCAT (siLYCAT^{1}, siLYCAT^{2}) for 72 h. When examined by western blot, two bands were detected at ~35 and ~25 kDa, which is consistent with predictions made by mRNA expression of a long and short LYCAT isoform (Cao et al., 2004) (Figure 3.1.1A). Silencing of LYCAT with siLYCAT^{1} resulted in a robust decrease in both the short and long isoform; 77% and 46% knockdown, respectively. siLYCAT^{2} was also successful in reducing both LYCAT bands, with an 8% reduction in the short isoform and 59% reduction in the long isoform (Figure 3.1.1B). Since the knockdown efficiency was greatest with siLYCAT^{1}, we proceeded to conduct most of the experiments with siLYCAT^{1}, and repeated key experiments with siLYCAT^{2}.

3.1.2 LYCAT silencing using CRISPR Cas9 system

To explore an additional method of silencing LYCAT, through our collaborators at the University of Toronto, we developed an inducible CRISPR Cas9 system targeting LYCAT. The Salmena Lab generated for us MDA-MB-231 cells that stably express the Cas9 recombinase. These cells were then modified by the stable insertion of doxycycline-inducible expression of 3 different guide

RNAs (gRNA) targeting LYCAT. To test the knockdown efficiency of this system, I treated cells with 0.1 μg/mL or 1 μg/mL doxycycline for 5 days. Upon testing the 3 different cell lines, I found that gRNA2 was the only cell line that resulted in a significant reduction in LYCAT levels (Figure 3.1.2). Further, the 1 μg/mL doxycycline induction resulted in greater knockdown of LYCAT compared to the 0.1 μg/mL treatment (Figure 3.1.2D-E). Thus, these results show that the CRISPR Cas9 cells are able to effectively knockdown LYCAT.

3.2 LYCAT silencing impacts EGFR phosphorylation and degradation differently in each cell type

3.2.1 LYCAT silencing increases EGF-stimulated EGFR phosphorylation in ARPE-19 cells

Previously, our work found that LYCAT silencing altered transferrin receptor internalization in ARPE-19 cells (Bone et al., 2017). Therefore, I wanted to determine whether LYCAT silencing would alter total EGFR levels and its signaling. In order to examine whether EGFR signaling was affected by LYCAT silencing, I utilised ARPE-19 cells, a non-transformed cell line. Cells were transfected with NT siRNA or siLYCAT[1] for 72 h. Next, I incubated cells in 2 mL of serum free media for 1 h, followed by EGF stimulation for 5 minutes. Lysates were probed for total EGFR levels and phospho-EGFR (Y1068) levels (Figure 3.2.1A). We observed no change in total EGFR levels but a slight increase in phospho-EGFR levels (Figure 3.2.1B-C). These results suggest that EGFR signalling remains intact despite perturbations in LYCAT expression.

3.2.2 LYCAT silencing reduces EGF-stimulated EGFR phosphorylation in MDA-MB-231 cells

To determine whether the effect of LYCAT silencing on EGFR signalling was the same in a cancerous cell line, we measured total and phospho-EGFR in MDA-MB-231 cells. While there

appears to be a loss of total EGFR upon LYCAT silencing, the effect was not significant (Figure 3.2.2C). Thus, in MDA-MB-231 cells there may be a change in total levels, but we cannot conclude this definitively at this time. However, we observed a definite loss of EGFR phosphorylation upon LYCAT silencing (Figure 3.2.2B). These results suggest that EGFR activation may be affected by LYCAT silencing in MDA-MB-231 cells.

3.2.3 LYCAT silencing may impact EGFR degradation in MDA-MB-231 cells

The possibility that EGFR levels are reduced in LYCAT silenced cells suggests that EGFR membrane traffic and degradation may be regulated by LYCAT. Upon binding EGF, EGFR undergoes dimerization, internalization, and a fraction of ligand-bound EGFR is sorted to the lysosome for degradation, leading to signal termination (Goh & Sorkin, 2013). In order to determine the effect of LYCAT silencing on EGFR degradation, I performed an EGFR degradation assay. Cells were transfected for 72 h with non-targeting siRNA or siLYCAT. Following transfection, cells were serum starved for 1 h. After serum starvation, cells were stimulated with 100 ng/mL EGF for 0, 30, 60 and 90 min; whole cell lysates were prepared. This concentration of EGF is sufficient for inducing to EGFR degradation in certain cell lines (Antonescu et al., 2010). Consistent with previous findings (Tubbesing et al., 2020), the receptor was not degraded in MDA-MB-231 cells transfected with NT siRNA. Total EGFR levels remain elevated after 90 min of EGFR stimulation (Figure 3.2.3). Total EGFR levels were slightly reduced in siLYCAT treated cells compared to control. Though not significant, it appears as though LYCAT silencing did alter EGFR degradation (Figure 3.2.3B). However, these results may suggest that a minor role for LYCAT in suppressing EGFR degradation could be revealed if this experiment was further repeated. These results

indicate that LYCAT silencing may not have a robust effect on receptor degradation in MDA-MB-231 cells.

3.3 LYCAT silencing suppresses EGF-stimulated Akt phosphorylation

3.3.1 LYCAT silencing suppresses EGF-stimulated Akt phosphorylation in ARPE-19 cells

In order to determine whether LYCAT silencing suppresses EGF-stimulated phosphorylation of Akt, I transfected ARPE-19 cells for 72 h with non-targeting siRNA (NT siRNA) or siLYCAT (siLY[1]). Following transfection, cells were serum starved for 1 h followed by 0 or 5 min EGF stimulation. After stimulation, whole cell lysates were prepared and used for Western blot analysis. I used a pan-phospho-Akt antibody that recognizes several Akt isoforms to probe for phosphorylation of Akt. EGF stimulation caused an increase in the activation and phosphorylation of Akt relative to basal levels (Figure 3.31.A). However, upon LYCAT silencing, there was a reduction in the phosphorylation of Akt compared to control. I observed an overall 17% decrease in phospho-Akt (S473) levels (Fig. 3.3.1B). To determine whether the reduction in phosphorylation was in fact a result of less activation rather than lower total Akt protein levels, I normalized phospho-Akt levels to total Akt levels. Relative to total Akt, there was a 31% decrease in the phosphorylation of Akt upon LYCAT silencing (Figure 3.3.1C). These results suggest that LYCAT silencing selectively inhibits EGF-stimulated Akt phosphorylation.

After determining that LYCAT silencing suppresses Akt phosphorylation in ARPE-19 cells, I wanted to test whether LYCAT silencing specifically impacted the Akt isoforms, Akt1 and Akt2. Since the different Akt isoforms preferentially bind to different phosphoinositides, we wanted to examine whether there were any differences in phosphorylation level after LYCAT silencing. In

order to determine the effect on specific Akt isoforms, we utilized isoform specific phospho-Akt antibodies to observe the effect of LYCAT silencing on phosphorylation. Lysates were probed with anti-pAkt1 (S473) and anti-pAkt2 (S474) antibodies (Figure 3.3.1E-L). Our results showed a 35% decrease in Akt1 phosphorylation and a 79% decrease in Akt2 phosphorylation normalized to total protein levels. These results suggest that LYCAT silencing inhibits EGF-stimulated phosphorylation of both Akt isoforms, with Akt2 phosphorylation appearing to be more inhibited.

3.3.2 LYCAT silencing suppresses EGF-stimulated Akt phosphorylation in MDA-MB-231 cells

Keeping with the intention of comparing a control cell line to a cancerous cell line, I next examined the effect of LYCAT silencing on Akt phosphorylation in MDA-MB-231 cells. Of note, LYCAT silencing in MDA-MB-231 cells led to a reduction in EGF-stimulated EGFR phosphorylation. Hence, these cells will not allow me to resolve a role for LYCAT specifically in the activation of Akt, but this cancer cell line does allow study of the function of LYCAT in cancer cell signaling and physiology. Cells were transfected with NT siRNA, or siLYCAT[1]. After 72 h of transfection, cells were serum starved for 1 h followed by subsequent EGF stimulation for 0, 5 or 10 min. After stimulation, cells were lysed and whole cell lysates were prepared. Using pan-phospho-Akt and pan-total-Akt levels antibodies, Western blot analysis showed a 71% reduction in absolute pAkt levels, and 66% reduction when normalized to total Akt levels (Figure 3.3.2A-D). These results suggest that LYCAT silencing impacts Akt activation and phosphorylation in MDA-MB-231 cells. Next, I further examined the effect of LYCAT silencing on Akt1 and Akt2, using isoform specific antibodies. The western blot results showed a 70% decrease in pAkt1 levels (Figure 3.3.2G) and

a 62% decrease in pAkt2 levels (Figure 3.3.2K), relative to total levels. These results suggest that activation of Akt suppressed in LYCAT silenced cells.

3.4. LYCAT silencing suppresses specific substrates downstream of Akt

3.4.1 LYCAT silencing suppresses pTSC2 and pGSK3ß in ARPE-19 cells

Since I previously observed a decrease in the phosphorylation of Akt, I next wanted to see if this effect was observed on several known substrates downstream of Akt. To measure the effect on these specific targets, I used anti-phospho-TSC2 (T1462), anti-phospho-GSK3ß (S9) and anti-phospho-MDM2 (S166) antibodies. I observed a 47% decrease in phospho-TSC2 (Figure 3.4.1C) and a 34% decrease in phospho-GSK3ß (Figure 3.4.1G) when normalized to total levels. There was a 41% decrease in absolute phospho-MDM2 levels (Figure 3.4.1J). However, when normalized to total levels this effect was no longer seen. This suggests that in ARPE-19 cells, LYCAT silencing leads to loss of EGF-stimulated TSC2 and GSK3ß phosphorylation, as well as a loss of MDM2 protein levels.

3.4.2 LYCAT silencing suppresses pTSC2 and pGSK3ß in MDA-MB-231 cells

In order to measure the effect of LYCAT silencing on the phosphorylation of substrates downstream of Akt in MDA-MB-231 cells, I re-probed previously made samples for phospho-TSC2, phospho-GSK3ß and phospho-MDM2. In LYCAT silenced cells, there was a significant decrease in the phosphorylation of all three substrates (Figure 3.4.2). When normalized to total protein levels, there was a 68% decrease in phospho-TSC2 levels (Figure 3.4.2C) and a 46% decrease in phosoho-GSK3ß levels (Figure 3.4.2G). Consistent with what I observed in ARPE-19

cells, although there was a significant decrease in absolute phospho-MDM2 levels, there was also a significant decrease in total MDM2 levels upon LYCAT silencing. When normalized to total MDM2, there was no difference in the phosphorylation of MDM2 in LYCAT silenced cells compared to control (Figure 3.4.2K). These results suggest that LYCAT silencing impacts the ability of Akt to phosphorylate specific downstream targets, in particular GSK3b and TSC2.

3.5. LYCAT silencing impairs mRNA translation and cell proliferation

3.5.1 LYCAT silencing inhibits protein synthesis

Since the PI3K-Akt pathway is involved in regulating protein synthesis and Akt activation was found to be impaired in LYCAT silenced cells, I wanted to test whether silencing had an effect on mRNA translation. To do this, I performed a puromycin incorporation assay. Puromycin is a tyrosyl-tRNA mimic that blocks translation by labelling and releasing elongating polypeptide chains from translating ribosomes. Puromycylated nascent peptides can then be detected through Western blot analysis using anti-puromycin antibodies. MDA-MB-231 cells were transfected for 72 h with non-targeting siRNA or siRNA targeting LYCAT, or left untransfected as a control. Upon Western blot analysis, I observed a 44% reduction in protein puromycylation upon LYCAT silencing, which is consistent with the reduction in signaling by the Akt pathway in these cells. As a control, cells treated with cycloheximide, an inhibitor of protein synthesis, exhibited a robust reduction of protein puromycylation. These results suggest that LYCAT silencing is involved in regulating protein synthesis, although a significant level of protein synthesis still occurs in LYCAT-silenced cells.

3.5.2 LYCAT silencing inhibits cell proliferation and increases apoptosis

Since the PI3K-Akt pathway is known to be involved in cell proliferation and survival, I next sought to determine whether LYCAT silencing would have an effect on cell growth. To measure the effect of LYCAT silencing on cell proliferation and apoptosis, I used the Incucyte SX5 Live Cell Analysis system to image cells in an environmentally controlled chamber over long periods of time and two gene silencing methods. Firstly, MDA-MB-231 cells were transfected with non-targeting siRNA or siLYCAT[1]. After the second round of transfection, optiMEM was removed and cells were washed once with PBS. Next, media with CellTox Green was added to the cells. Phase contrast and green fluorescent channel images were taken over the course of 72 h with images acquired every 30 min. While control cells grew and increased in confluency over 72 h, the LYCAT silenced cells displayed an impairment in cell growth. We observed a 21% decrease in phase confluence at 72 h, upon LYCAT silencing, as well as an 55% increase in CellTox Green count relative to phase confluence (Figure 3.5.2A-C). These results suggest that LYCAT silencing increases cell death and may also impair cell proliferation.

Since these experiments required prolonged LYCAT silencing, I also used the CRISPR cell line obtained from the Salmena lab as an additional experimental model. 4 days after initial seeding, cells were washed with PBS and new media containing CellTox green dye was added to the cells. Brightfield phase contrast and green channel images were taken every 30 min over 72 h. MDA-MB-231 Cas9 control cells with and without doxycycline treatment, increased in phase confluence over the 72 h period. MDA-MB-231 Cas9 tet gLCLAT1-2 cells treated with 1 µg/mL doxycycline exhibited impaired cell growth as indicated by overall percent phase confluence when compared to control conditions (Figure 3.5.2D-F). However, the difference in CellTox Green

object count between conditions was negligible (data not shown). Taken together with the results of the siRNA silencing of LYCAT, these results suggest that LYCAT has a role to play in regulating cell proliferation and survival.

CHAPTER 3 FIGURES

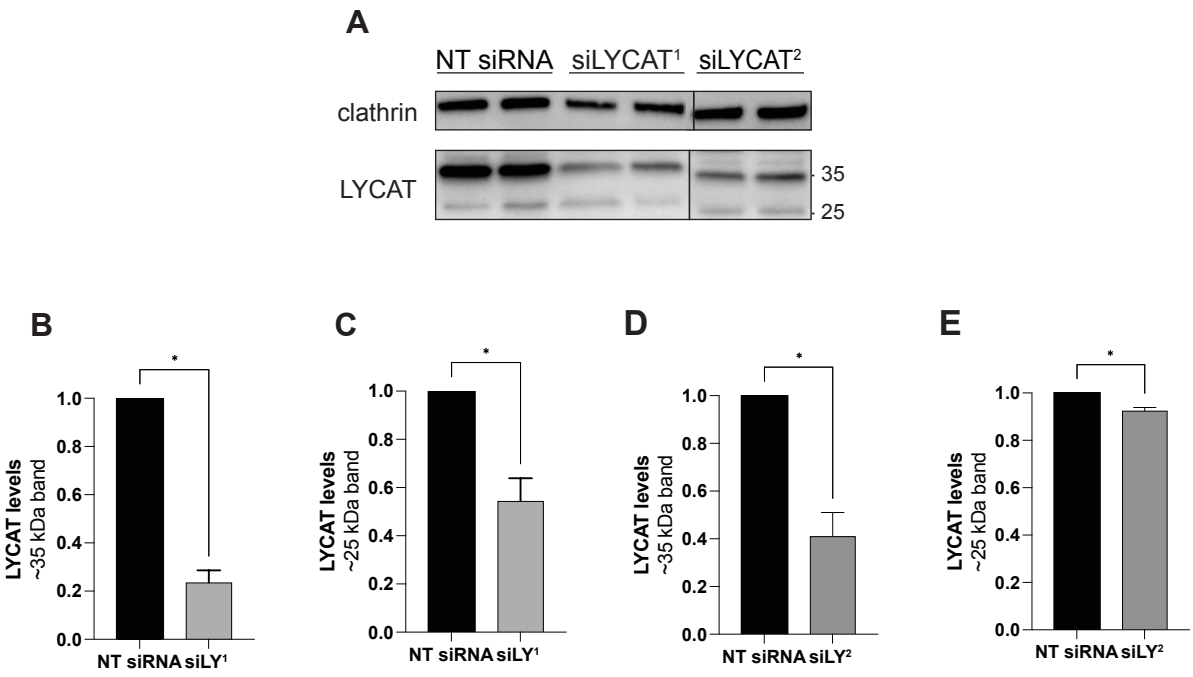

Figure 3.1.1 LYCAT silencing by siRNA is efficient in MDA-MB-231 cells.

MDA-MB-231 cells were transfected with non-targeting siRNA or siRNA targeting LYCAT (siLYCAT^1 or siLYCAT^2). Prior to cell lysis, cells were serum starved for 1 h, then subsequently stimulated with EGF (5 ng/mL) for 5 min. Whole cell lysates were prepared and subjected to Western blot analysis. **A)** Representative immunoblots probing for LYCAT and housekeeping protein, clathrin, are shown. Blots show two LYCAT bands at ~35 and ~25 kDa. **B-E)** Quantitative measurements of LYCAT levels relative to clathrin are displayed as mean ± SEM (n=3). Unpaired *t* test, *p <0.05.

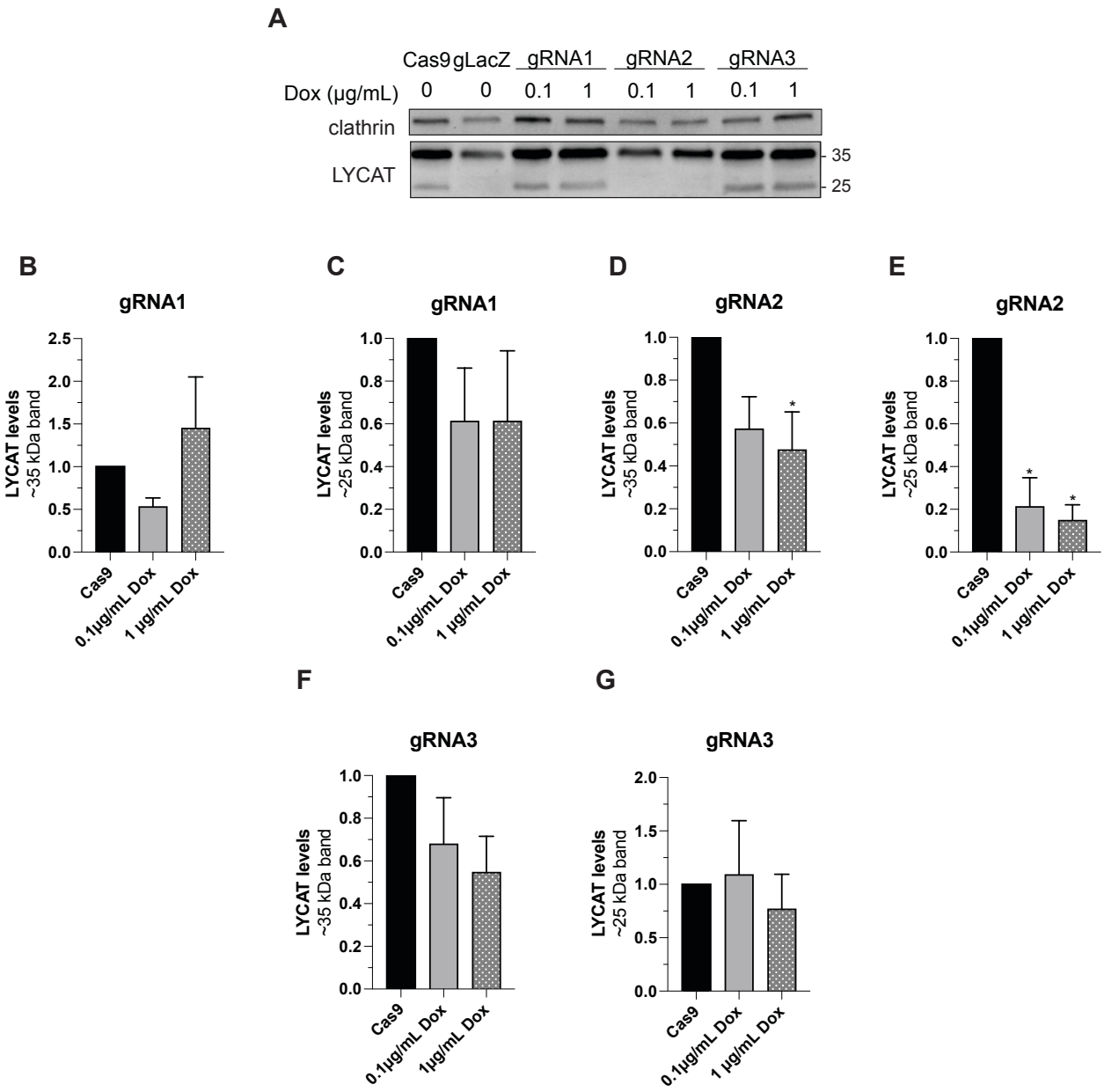

Figure 3.1.2 LYCAT silencing by an inducible CRISPR Cas9 system is efficient in MDA-MB-231 cells.

MDA-MB-231 cells stably expressing Cas9 with three inducible gRNAs targeting LYCAT were utilised. Cells were treated with or without doxycycline of differing concentrations (0.1 µg/mL or 1 µg/mL) for 5 days. Following doxycycline induction, whole cell lysates were prepared and subjected to Western blot analysis. **A)** Representative immunoblots probing for LYCAT and housekeeping protein, clathrin, are shown. **B-G)** Quantitative measurements of the levels of two LYCAT isoforms (~35 and ~25 kDa) normalized to clathrin for each gRNA are represented as mean

± SEM (n=3). Two-way ANOVA with Tukey's multiple comparison test, only panels with a p value over the threshold of $p < 0.05$, are denoted with an asterisk on the graph.

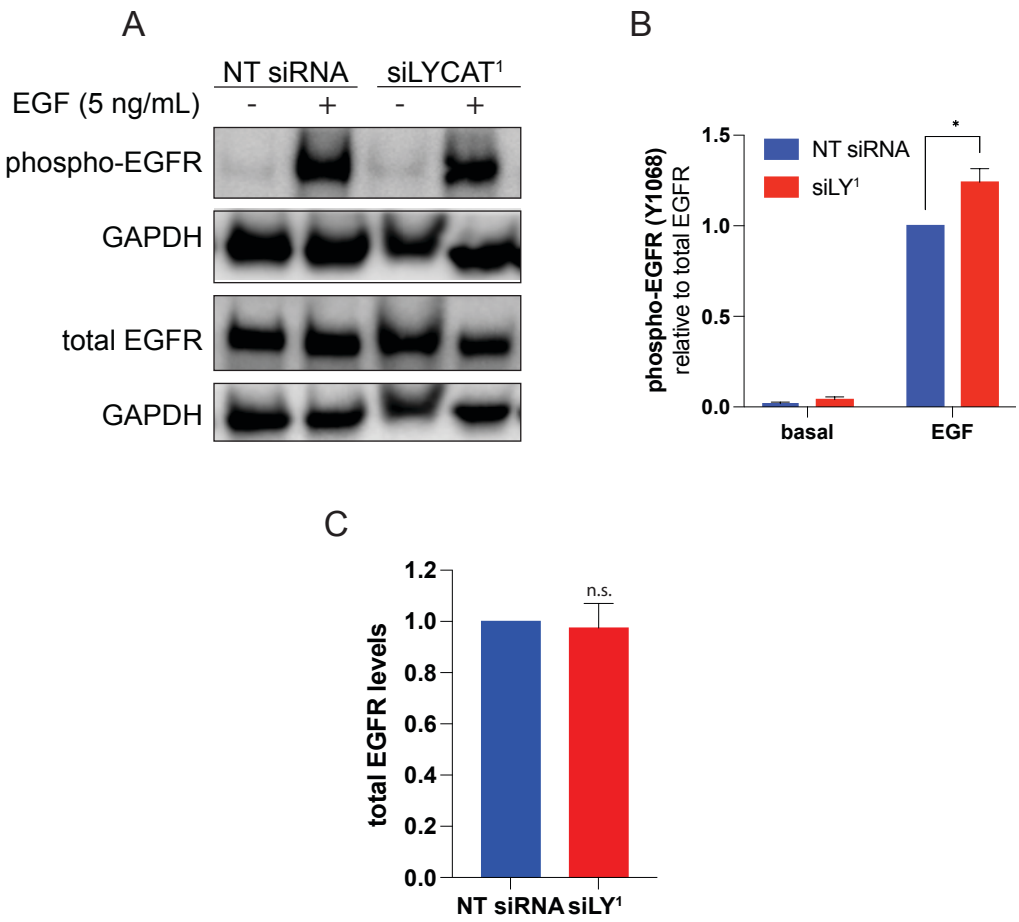

Figure 3.2.1 LYCAT silencing increases EGFR phosphorylation in ARPE-19 cells.

ARPE-19 cells were transfected with non-targeting siRNA or siRNA targeting LYCAT (siLYCAT[1]). Following transfection, cells were serum starved for 1 h and subsequently stimulated with EGF (5 ng/mL) for 5 min. Whole cell lysates were prepared and subjected to Western blot analysis. **A)** Representative immunoblots probing for phospho-EGFR (Y1068), total EGFR and GAPDH are shown. **B)** Quantitative measurements represented as mean ± SEM of phospho-EGFR (Y1068) levels relative to total EGFR (n=4), two-way ANOVA with Tukey's multiple comparison test, *p <0.05. **C)** Quantitative measurements of total EGFR levels represented as mean ± SEM (n=4), unpaired *t* test.

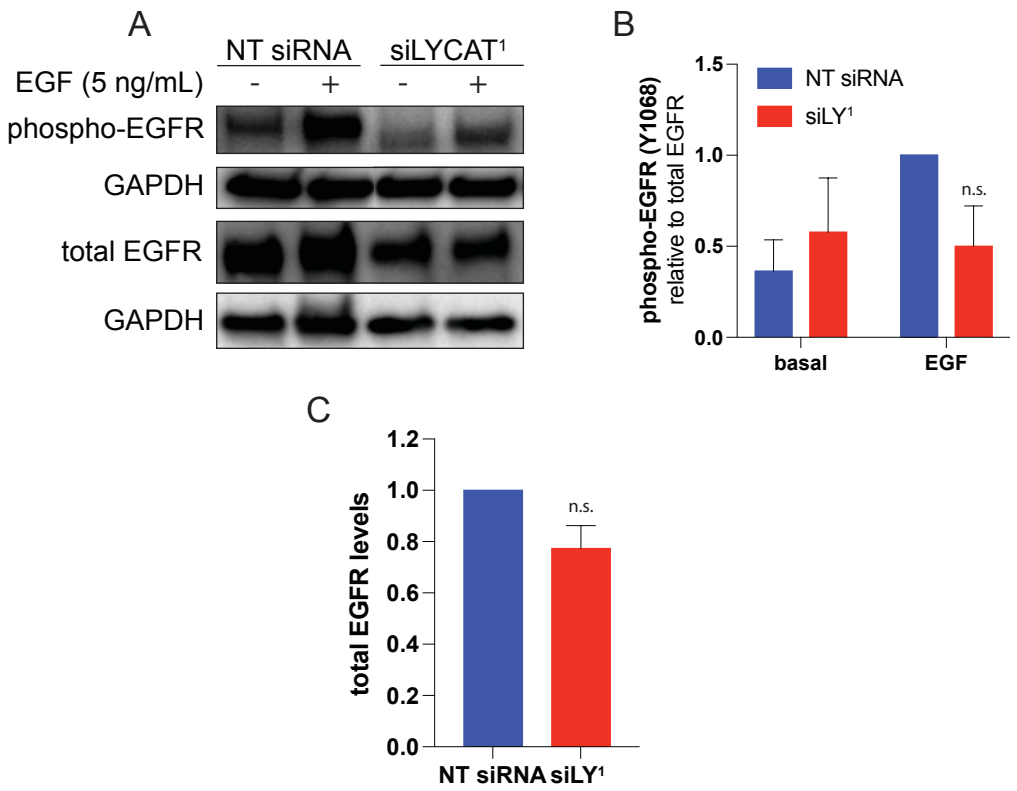

Figure 3.2.2 LYCAT silencing reduces EGFR phosphorylation in MDA-MB-231 cells.

MDA-MB-231 cells were transfected with non-targeting siRNA or siRNA targeting LYCAT (siLYCAT[1]). Following transfection, cells were serum starved for 1 h and subsequently stimulated with EGF (5 ng/mL) for 5 min. Whole cell lysates were prepared and subjected to Western blot analysis. **A)** Representative immunoblots probing for phospho-EGFR (Y1068), total EGFR and GAPDH are shown. **B)** Quantitative measurements represented as mean ± SEM of phospho-EGFR (Y1068) levels relative to total EGFR (n=3), two-way ANOVA with Tukey's multiple comparison test. **C)** Quantitative measurements of total EGFR levels represented as mean ± SEM (n=3), unpaired *t* test. Results in panels B and C reported no significant difference between conditions.

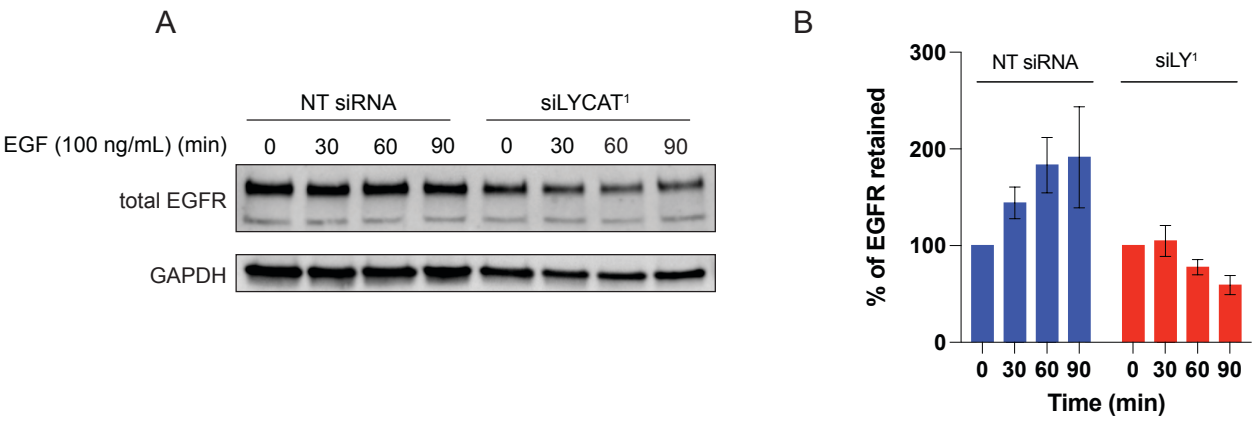

Figure 3.2.3 LYCAT silencing does not impact EGFR degradation in MDA-MB-231 cells.

MDA-MB-231 cells were transfected with non-targeting siRNA or siRNA targeting LYCAT (siLYCAT[1]). After 72 h of transfection, cells were serum starved for 1 h followed by EGFR stimulation (100 ng/mL) for 0, 30, 60 or 90 min. After serum stimulation, whole cell lysates were prepared and subjected to Western blot analysis. **A)** Representative immunoblots probing total EGFR and housekeeping protein, GAPDH, are shown **B)** Quantitative analysis represented as mean ± SEM of percent of EGFR retained relative to GAPDH levels, (n=3). Conditions were n.s.

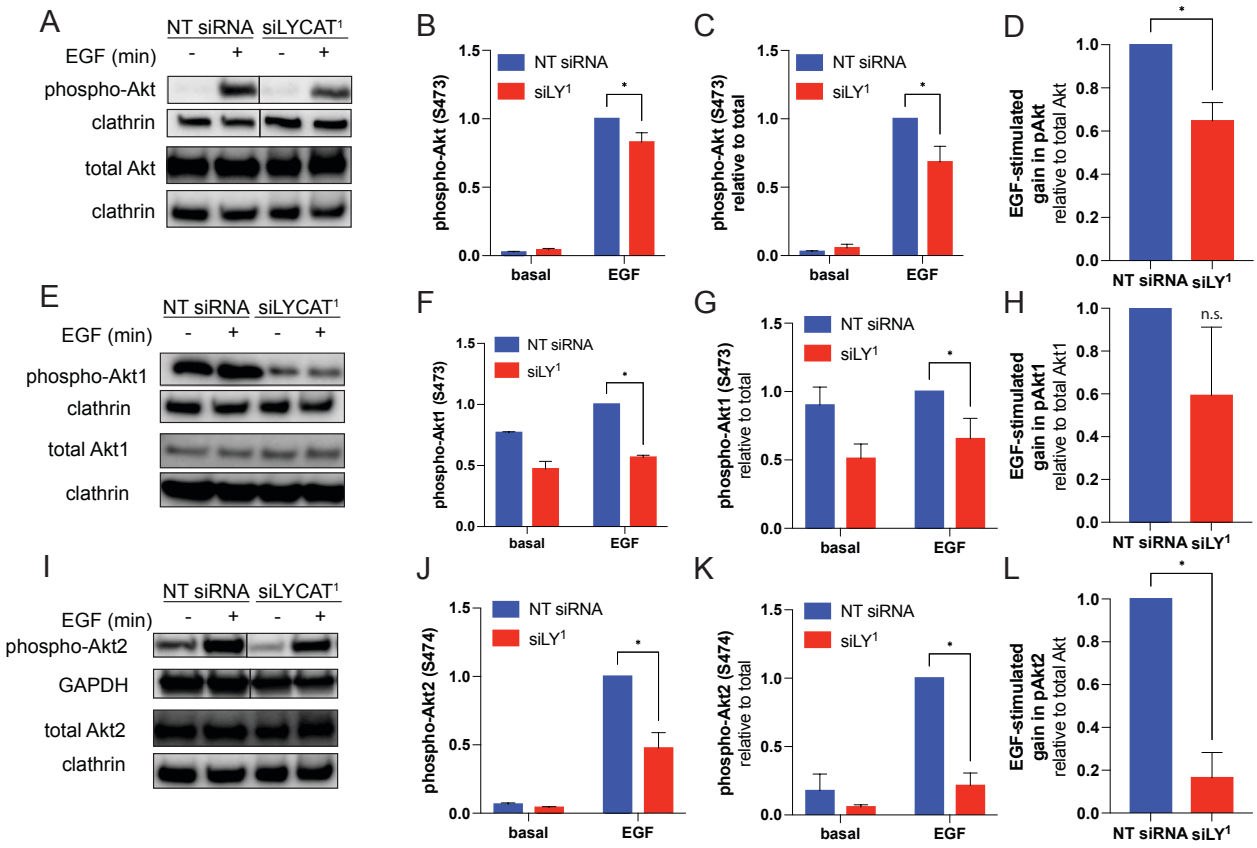

Figure 3.3.1 LYCAT silencing suppresses EGF-stimulated Akt phosphorylation in ARPE-19 cells

ARPE-19 cells were transfected with non-targeting siRNA or siRNA targeting LYCAT (siLYCAT[1]). After 72 h of transfection, cells were serum starved for 1 h followed by stimulation with EGF (5 ng/mL) for 5 or 10 min. Whole cell lysates were prepared and subjected to Western blot analysis. **A)** Representative immunoblots probing for phospho-Akt (S473), total Akt and housekeeping protein, clathrin. **B-D)** Quantitative measurements represented as mean ± SEM of absolute phospho-Akt (S473) levels, phospho-Akt (S473) levels relative to total Akt, and EGF-stimulated gain in phospho-Akt (S473) relative to total Akt, (n=3). **E)** Representative immunoblots probing for phospho-Akt1 (S473), total Akt1 and housekeeping proteins, GAPDH and clathrin. **F-H)** Quantitative measurements represented as mean ± SEM of absolute phospho-Akt1 (S473) levels, phospho-Akt1 (S473) levels relative to total Akt1, and EGF-stimulated gain in phospho-Akt1 (S473) relative to total Akt1, (n=3). **I)** Representative immunoblots probing for phospho-Akt2 (S474), total Akt2 and housekeeping proteins, GAPDH and clathrin. **J-L)** Quantitative measurements represented as mean ± SEM of absolute phospho-Akt2 (S474) levels, phospho-

Akt2 (S474) levels relative to total Akt2, and EGF-stimulated gain in phospho-Akt2 (S474) relative to total Akt, (n=3). All panels except for panels D, H and L were subjected to a two-way ANOVA with Tukey's multiple comparison test. Unpaired *t* tests were conducted for panels D, H and L, *p <0.05.

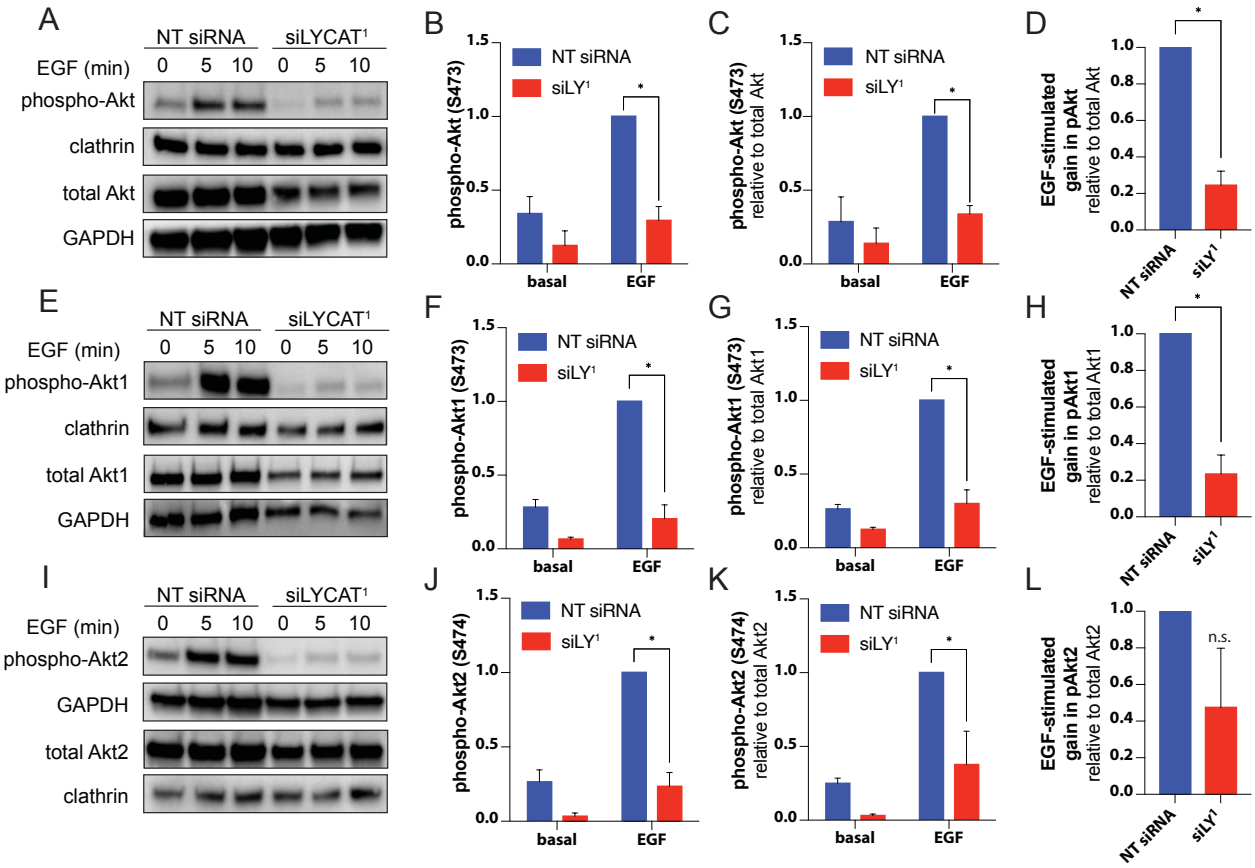

Figure 3.3.2 LYCAT silencing suppresses EGF-stimulated Akt phosphorylation in MDA-MB-231 cells

MDA-MB-231 cells were transfected with non-targeting siRNA or siRNA targeting LYCAT (siLYCAT[1]). After 72 h of transfection, cells were serum starved for 1 h followed by stimulation with EGF (5 ng/mL) for 5 or 10 min. Whole cell lysates were prepared and subjected to Western blot analysis. **A)** Representative immunoblots probing for phospho-Akt (S473), total Akt and housekeeping proteins, GAPDH and clathrin. **B-D)** Quantitative measurements represented as mean ± SEM of absolute phospho-Akt (S473) levels, phospho-Akt (S473) levels relative to total Akt, and EGF-stimulated gain in phospho-Akt (S473) relative to total Akt, (n=3). **E)** Representative immunoblots probing for phospho-Akt1 (S473), total Akt1 and housekeeping proteins, GAPDH and clathrin. **F-H)** Quantitative measurements represented as mean ± SEM of absolute phospho-Akt1 (S473) levels, phospho-Akt1 (S473) levels relative to total Akt1, and EGF-stimulated gain in phospho-Akt1 (S473) relative to total Akt1, (n=3). **I)** Representative immunoblots probing for

phospho-Akt2 (S474), total Akt2 and housekeeping proteins, GAPDH and clathrin. **J-L)** Quantitative measurements represented as mean ± SEM of absolute phospho-Akt2 (S474) levels, phospho-Akt2 (S474) levels relative to total Akt2, and EGF-stimulated gain in phospho-Akt2 (S474) relative to total Akt, (n=3). All panels except for panels D, H and L were subjected to a two-way ANOVA with Tukey's multiple comparison test. Unpaired *t* tests were conducted for panels D, H and L, *p <0.05.

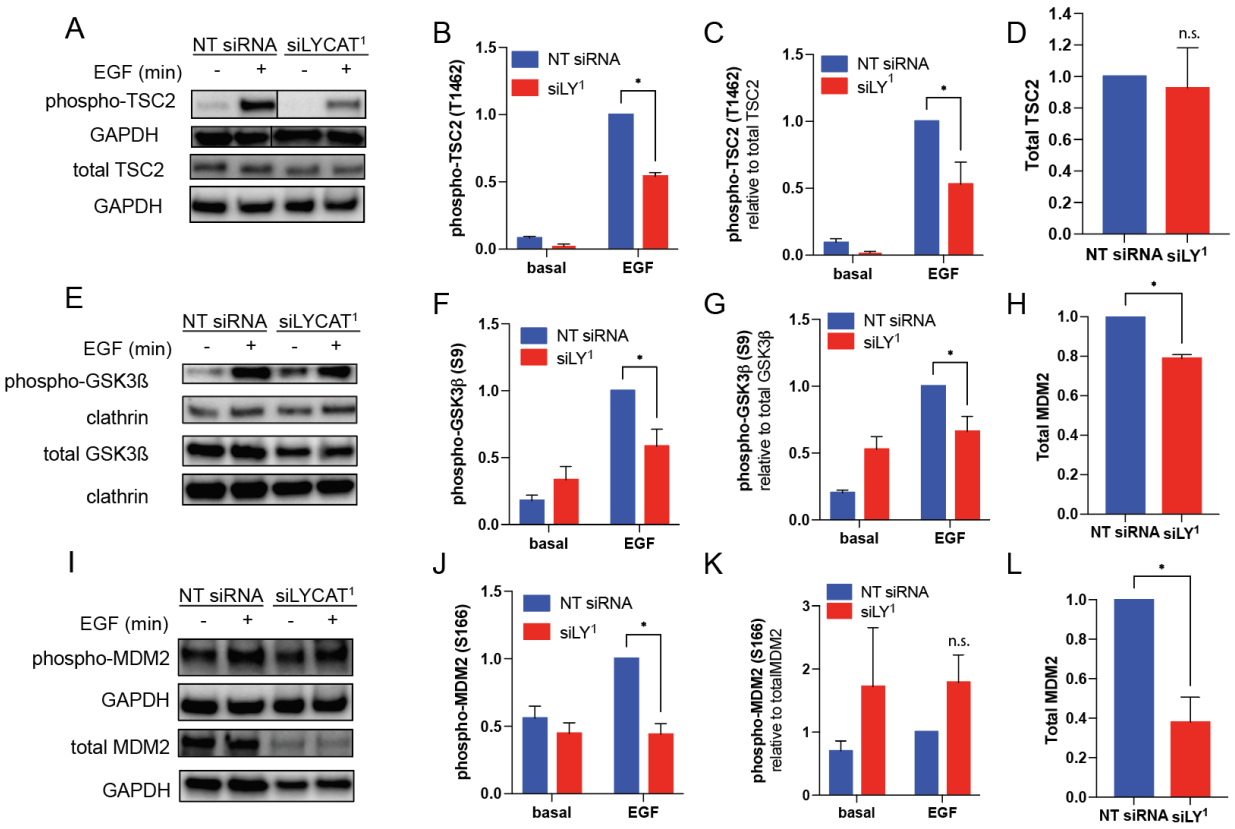

Figure 3.4.1 LYCAT silencing leads to a reduction in the phosphorylation of select substrates downstream of Akt in ARPE-19 cells.

ARPE-19 cells were transfected with non-targeting siRNA or siRNA targeting LYCAT (siLYCAT[1]). Prior to cell lysis, cells were serum starved for 1 h then subsequently stimulated with EGF (5 ng/mL) for 5 min. Whole cell lysates were prepared and subjected to Western blot analysis. **A)** Representative immunoblots probing for phospho-TSC2 (T1462), total TSC2 and housekeeping protein, GAPDH. **B-D)** Quantitative measurements represented as mean ± SEM of absolute phospho-TSC2 (T1462) levels, phospho-TSC2 (T1462) levels relative to total TSC2, and total TSC2 (n=3). **E)** Representative immunoblots probing for phospho-GSK3ß (S9), total GSK3ß and housekeeping proteins, GAPDH and clathrin. **F-H)** Quantitative measurements represented as mean ± SEM of absolute phospho-GSK3ß (S9) levels, phospho-GSK3ß (S9) levels relative to total GSK3ß, and total GSK3ß (n=3). **I)** Representative immunoblots probing for phospho-TSC2 (T1462), total TSC2 and housekeeping protein, GAPDH. **J-L)** Quantitative measurements represented as

mean ± SEM of absolute phospho-MDM2 (S166) levels, phospho- MDM2 (S166) levels relative to total MDM2, and total MDM2 (n=3). All panels except for panels D, H and L were subjected to a two-way ANOVA with Tukey's multiple comparison test. Unpaired *t* tests were conducted for panels D, H and L, *p <0.05.

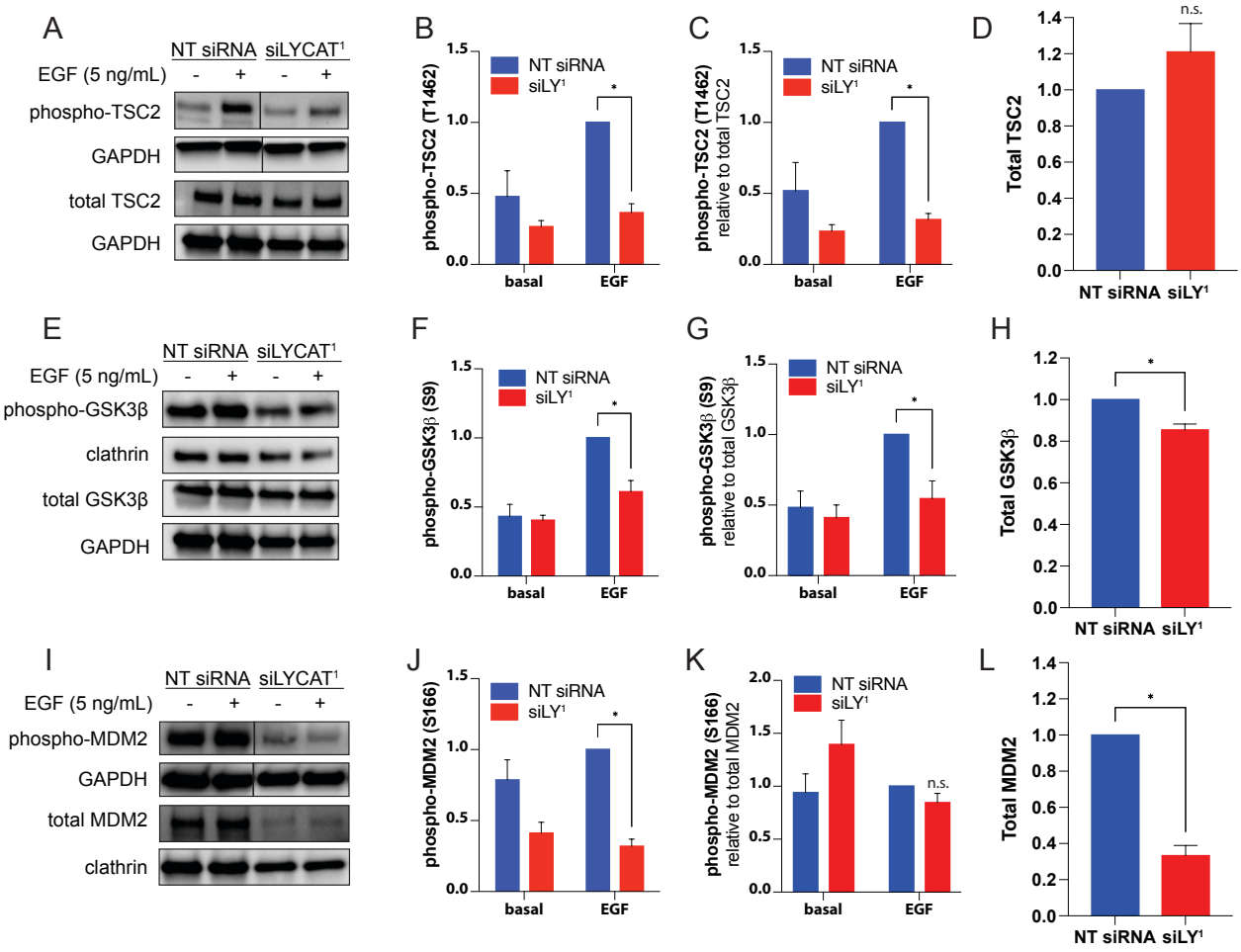

Figure 3.4.2 LYCAT silencing leads to a reduction in the phosphorylation of select substrates downstream of Akt in MDA-MB-231 cells.

MDA-MB-231 cells were transfected with non-targeting siRNA or siRNA targeting LYCAT (siLYCAT[1]). Prior to cell lysis, cells were serum starved for 1 h then subsequently stimulated with EGF (5 ng/mL) for 5 min. Whole cell lysates were prepared and subjected to Western blot analysis. **A)** Representative immunoblots probing for phospho-TSC2 (T1462), total TSC2 and housekeeping protein, GAPDH. **B-D)** Quantitative measurements represented as mean ± SEM of absolute phospho-TSC2 (T1462) levels, phospho-TSC2 (T1462) levels relative to total TSC2, and total TSC2 (n=3). **E)** Representative immunoblots probing for phospho-GSK3ß (S9), total GSK3ß and housekeeping proteins, GAPDH and clathrin. **F-H)** Quantitative measurements represented as mean ± SEM of absolute phospho-GSK3ß (S9) levels, phospho-GSK3ß (S9) levels relative to total GSK3ß, and total GSK3ß (n=3). **I)** Representative immunoblots probing for phospho-TSC2

(T1462), total TSC2 and housekeeping protein, GAPDH. **J-L)** Quantitative measurements represented as mean ± SEM of absolute phospho-MDM2 (S166) levels, phospho- MDM2 (S166) levels relative to total MDM2, and total MDM2 (n=3). All panels except for panels D, H and L were subjected to a two-way ANOVA with Tukey's multiple comparison test. Unpaired *t* tests were conducted for panels D, H and L, *p <0.05.

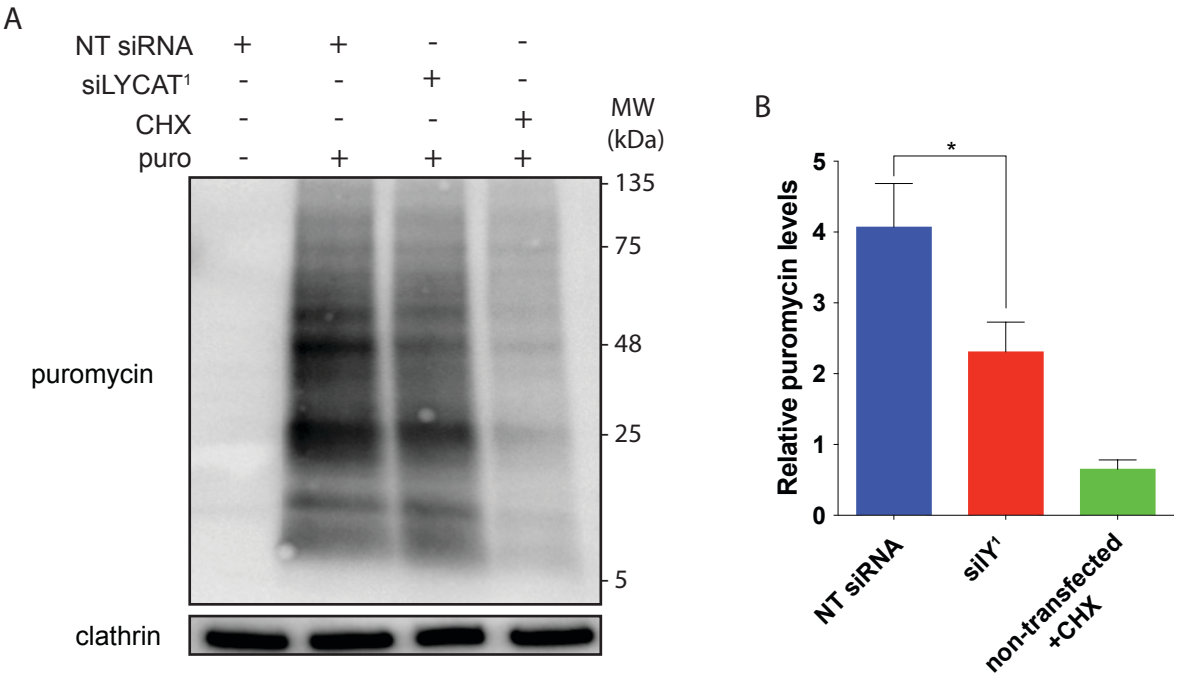

Figure 3.5.1 LYCAT silencing inhibits protein synthesis in MDA-MB-231 cells.

MDA-MB-231 cells were transfected with non-targeting siRNA, siRNA targeting LYCAT (siLYCAT[1]), or neither. Following transfection, cells were treated with cycloheximide (CHX) (10 µM) for 20 min and puromycin (10 µg/mL) for 10 min, as indicated. Whole cell lysates were prepared and subjected to Western blot analysis. **A)** Representative immunoblots probing puromycin and clathrin are shown. **B)** Quantitative measurements represented as mean ± SEM of puromycin levels relative to clathrin in NT siRNA, siLYCAT[1] and non-transfected cells treated with CHX (n=3), unpaired *t* test, *p <0.05.

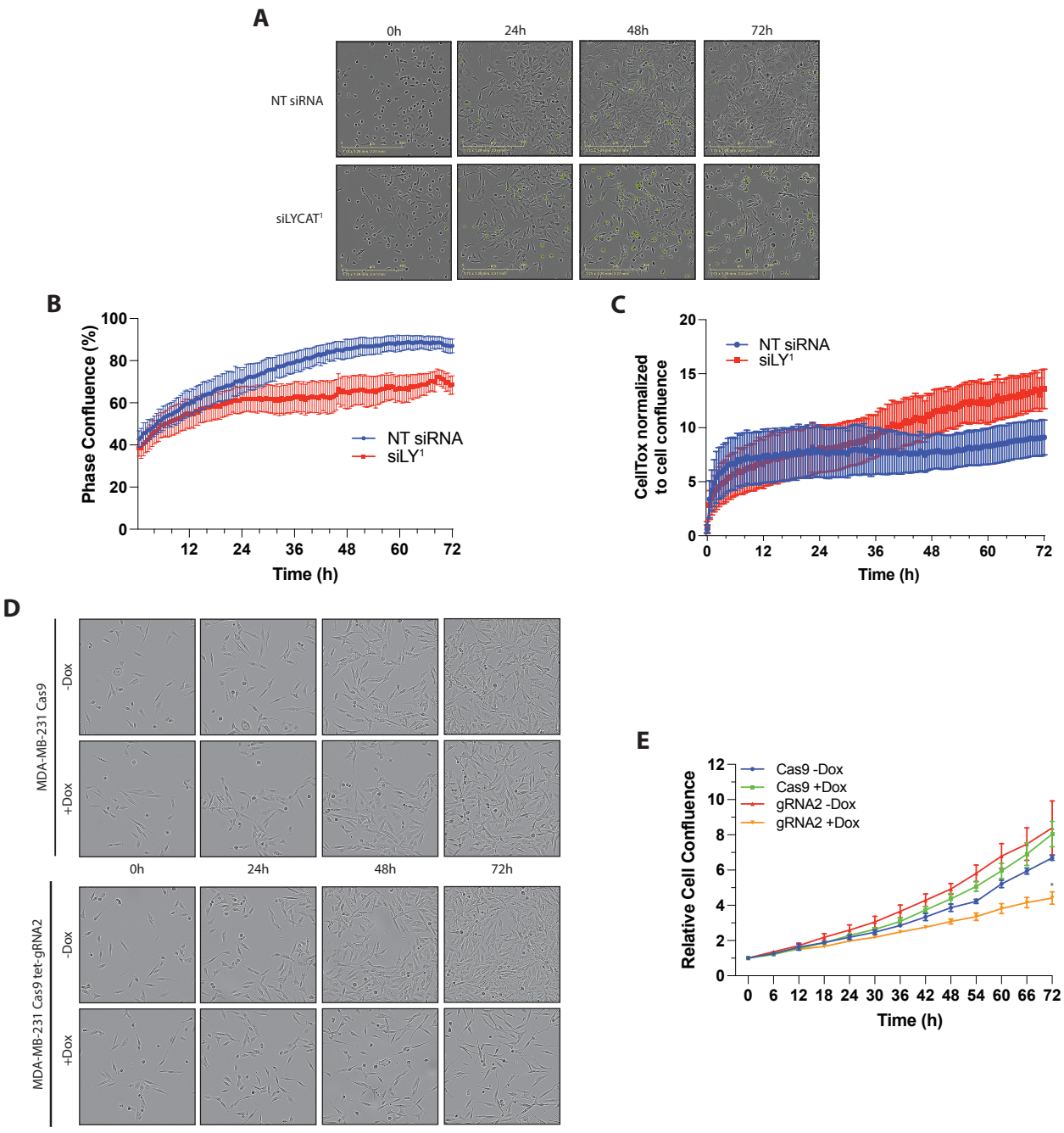

Figure 3.5.2 LYCAT silencing reduces cellular abundance in MDA-MB-231 cells.

A-D) MDA-MB-231 cells were transfected with non-targeting siRNA or siRNA targeting LYCAT (siLYCAT[1]). Following the second round of transfection, time-lapse images of the cells were taken every 30 min for 72 h using the Incucyte SX5. **A)** Representative images from the time-lapse recordings at 0, 24, 48 and 72 h are shown. **B)** Quantitative measurements of phase confluence

(%) over time (h) are displayed as mean ± SEM (n=4). **C)** Quantitative measurements of CellTox count (per image) normalized to cell confluence are displayed as mean ± SEM (n=4). **D-F)** MDA-MB-231 cells stably expressing Cas9 with an inducible gRNA targeting LYCAT were treated with 1 ug/mL doxycycline for 3 days. Cells were ten re-seeded and placed in the Incucyte SX5 where time-lapse recording of the cells were taken every 30 min for 72 h. **D)** Representative images from the time-lapse recording at 0, 24, 28 and 72 h are shown. **E)** Quantitative measurements of phase confluence relative to initial confluence are displayed as mean ± SEM (n=3), two-way ANOVA with Tukey's multiple comparison test, *p <0.05.

CHAPTER 4: DISCUSSION

4.1 Effects of LYCAT silencing on EGFR signaling are cell line dependent

Previously, our lab showed that LYCAT silencing altered endocytosis and transferrin receptor uptake in ARPE-19 cells (Bone et al., 2017). We then wanted to further explore whether LYCAT silencing would impact total EGFR levels and EGFR signaling. In ARPE-19 cells, there was no change in total EGFR levels between conditions (Figure 3.2.1C). Looking at EGFR signaling, we found that there was a slight increase in the phosphorylation of EGFR upon LYCAT silencing (Figure 3.2.1B). Similarly, in MDA-MB-231 cells, there was no significant difference in total EGFR levels between control and LYCAT silenced cells (Figure 3.2.2C). However, additional experiments may reveal a significant change in total EGFR levels. When we measured phospho-EGFR levels, we saw that there was a slight decrease in EGFR signaling, though not significant (Figure 3.2.2B). MDA-MB-231 cells are known for overexpressing EGFR, so I reasoned that the cell specific differences could perhaps be due to levels of EGFR and their trafficking and degradation.

Activation of EGFR upon ligand binding, leads to receptor internalization, ubiquitination by E3 ligases and traffic to the lysosome, ultimately leading to downregulation of the receptor. EGFR is internalized via CME and recycled to the EE where it can be sorted for degradation. The ESCRT machinery sorts ubiquitinated EGFR onto the intraluminal vesicles of maturing endosomes and further, fusion of the late endosome with lysosomes leads to the degradation of EGFR (Tomas et al., 2014). To elucidate whether LYCAT silencing had an effect on receptor degradation, I performed an EGFR degradation assay. In MDA-MB-231 cells, when control cells are treated with 100 ng/mL EGF for 90 minutes, total EGFR levels remain elevated, indicating no receptor degradation (Figure 3.2.3); this is consistent with previous findings (Tubbesing et al., 2020). When

we silenced LYCAT in these cells, we saw no effect on EGFR degradation. EGFR remained intact and there was no significant difference in total EGFR levels. This suggests that altered EGFR degradation is perhaps not the reason for the observed reduction in EGFR signaling, in LYCAT silenced cells. Another possibility is that EGFR has a preference to reside intracellularly in LYCAT-silenced MDA-MB-231 cells. EGF-stimulation causes the receptor to internalize and accumulate intracellularly without being degraded. In MDA-MB-231 cells, EGFR is strongly recruited to CCPs following EGF stimulation (Mutch et al., 2014). Perhaps cell surface EGFR levels are impacted by LYCAT silencing. Cell surface EGFR levels should be measured in MDA-MB-231 cells to better understand the mechanism by which LYCAT effects EGFR signaling.

4.2 LYCAT controls PI3K-Akt signaling

Using both pan-isoform and isoform-specific antibodies, we found that LYCAT silencing impaired PI3K-Akt signaling in ARPE-19 cells. LYCAT silencing was able to reduce the phosphorylation of Akt1 and Akt2. Interestingly, the magnitude at which LYCAT silencing perturbed activation was different between the two Akt isoforms. Our results showed a greater effect on phospho-Akt2, with a 79% reduction in phospho-Akt2 levels and a 35% reduction in phospho-Akt1 levels, relative to total levels (Figure 3.3.1). The Akt isoforms are known to preferentially bind to specific PIPs; Akt1 binds $PI(3,4,5)P_3$ while Akt2 binds $PI(3,4)P_2$ (Liu et al., 2018). In ARPE-19 cells, it seems as though there is a preference for LYCAT to act on the activation of Akt2 rather than Akt1. Perhaps this effect is due to altered SHIP2-dependent production of $PI(3,4)P_2$. SHIP2 is localized to CCPs upon EGFR activation (Cabral-Dias et al., 2022; Nakatsu et al., 2010). It is possible that SHIP2 localization and function is altered by LYCAT-silencing. Total internal reflection fluorescence

microscopy images of cells expressing GFP-SHIP2 and clathrin-mRP as described in (Nakatsu et al., 2010), may be able to tell us whether LYCAT silencing affects SHIP2 localization to CCPs.

When measuring the effect of LYCAT silencing on Akt activation in MDA-MB-231 cells, we observed a decrease in pan and isoform specific Akt phosphorylation. Phosphorylation of Akt1 and Akt2, was perturbed by LYCAT silencing at a similar magnitude. We saw a 71% decrease in relative phospho-Akt1 levels and a 66% decrease in relative phospho-Akt2 levels (Figure 3.3.2). However, when we compared the effect on Akt phosphorylation in the two different cell lines, we found that there was a greater effect in MDA-MB-231 cells compared to ARPE-19. LYCAT silencing resulted in a 66% reduction of relative phospho-Akt levels in MDA-MB-231 cells (Figure 3.3.2), while ARPE-19 cells only saw a 31% decrease (Figure 3.3.1). The magnitude, or extent to which LYCAT may affect Akt signaling in the two cell lines, may be explained by the effect on EGFR signaling that was previously discussed. Perhaps, the reason as to why there is a greater reduction in MDA-MB-231 cells is because LYCAT regulates not only PI3K-Akt signaling, but EGFR signaling at the level of receptor phosphorylation as well. I propose that LYCAT silencing has a greater effect in MDA-MB-231 cells because EGFR phosphorylation is also impaired, meaning there is reduced recruitment of adaptor proteins necessary to activate PI3K and produce $PI(3,4,5)P_3$. To test this, we could measure phosphorylated Gab1 levels in LYCAT silenced cells. This may also help us to address a critical component that is missing in our understanding: what is happening upstream of PIP_3? How does LYCAT silencing affect events after EGFR signaling and before PIP_3 synthesis. Additionally, the change in acyl chain profile, lower levels, and altered localization of $PI(4,5)P_2$ will also impair $PI(3,4,5)P_3$ conversion. To test this, we could measure PIP levels in LYCAT

silenced MDA-MB-231 cells through radiolabelling and high-performance liquid chromatography (HPLC) and detect acyl profile through mass spectrometry. We can investigate PIP localization upon LYCAT silencing in MDA-MB-231 cells, through the use of PIP specific probes, such as PH-PLCδ which binds PI(4,5)P_2 (Garcia et al., 1995). Another aspect that would be important to address is how LYCAT, an ER-localized protein, is able to affect PM PIPs. LYCAT localizes to PIS-containing vesicles, which have been shown to make transient contacts with the plasma membrane (Kim et al., 2011). Thus, further work should investigate the role of LYCAT at ER-PM contact sites.

In both cell lines, I observed a decrease in the phosphorylation of Akt substrates, TSC2 and GSK3ß, upon LYCAT silencing. In ARPE-19 cells, I saw a 47% reduction in relative phospho-TSC2 levels and a 34% decrease in relative phospho-GSK3ß levels (Figure 3.4.1) In MDA-MB-231 cells, there was a 68% decrease in relative phospho-TSC2 levels and a 46% decrease in relative phospho-GSK3ß levels (Figure 3.4.2). Again, when we compare the effects seen in the two cell lines, I saw that the effect was greater in MDA-MB-231 cells. The effect on MDM2 varied slightly. Akt-mediated phosphorylation of MDM2 increases MDM2 stability by promoting nuclear entry (Chibaya et al., 2021) and inhibiting its self-ubiquitination (Feng et al., 2004). We observed a decrease in absolute phospho-MDM2 levels in both cell lines. When normalized to total levels, this effect was no longer present. This was because there was also a massive loss of total MDM2 upon LYCAT silencing. Therefore, normalizing phospho-MDM2 levels to total levels may not give us a clear understanding of how LYCAT regulates MDM2 activity. It would be useful to use subcellular fractionation to measure cytoplasmic and nuclear MDM2 levels. I suggest that the

drop in total levels is due to reduced MDM2 stability as a result of less Akt-mediated phosphorylation. However, MDM2 stability is not solely regulated by its Akt phosphorylation events. MDMX is a close homologue of MDM2 that plays an important role in stabilizing MDM2. Studies have shown that MDMX binds to MDM2 via their RING finger domains which may inhibit MDM2's self-ubiquitin ligase activity (Stad et al., 2000). Akt has also been shown to mediate the phosphorylation of MDMX at Ser367 (Lopez-Pajares et al., 2008). This phosphorylation leads to the stabilization of MDMX and subsequently, the stabilization of MDM2. Perhaps, LYCAT silencing destabilizes MDM2 by preventing Akt-mediated phosphorylation of both MDM2 and MDMX.

MDM2 and p53 form a negative feedback loop. The tumour suppressor, p53 induces the expression of MDM2, which in turn promotes the degradation of p53. More specifically, phosphorylation of MDM2 leads to the translocation of MDM2 from the cytoplasm into the nucleus. Once MDM2 has gained nuclear entry, it is able to regulate p53, inactivating it (Mayo & Donner, 2001). Thus, a loss of MDM2 would result in less p53 degradation. This would mean that p53 is able to exert its tumour suppressing functions, promoting cell cycle arrest and apoptosis. Lysates should be probed for p53 levels to see whether LYCAT silencing has an effect on protein levels. Since there is a reduction in MDM2 levels upon LYCAT silencing, I predict that there would be an increase in p53 levels, which may also contribute to the effect on apoptosis discussed in the next section.

4.3 LYCAT controls protein synthesis, cell proliferation and apoptosis

In MDA-MB-231 cells, LYCAT silencing resulted in a reduction of protein synthesis compared to control non-targeting siRNA (Figure 3.5.1). As previously discussed, I observed a decrease in

phospho-TSC2 levels upon LYCAT silencing (Figure 3.4.2A-D). TSC1 and TSC2 function as a heterodimer to inhibit cell growth and proliferation by regulating the mTOR signaling pathway(Y. Li et al., 2004). TSC2 acts as a GAP for Rheb, promoting the conversion of Rheb-GTP to Rheb-GDP. In its active GTP-bound state, Rheb activates mTORC1 which stimulates the phosphorylation of ribosomal protein S6 kinase beta-1 (S6K) and eukaryotic translation initiation factor 4E binding protein 1(4E-BP1) (Yu et al., 2005). S6K and 4E-BP1 are involved in promoting protein synthesis (Choo et al., 2008). Thus, TSC2 is responsible for inactivating Rheb, which in turn inhibits mTORC1 and some aspects of protein synthesis. However, Akt-mediated phosphorylation of TSC2 prevents the hydrolysis of Rheb-GTP. This means that there is more active Rheb which allows for mTORC1 to become activated when Akt signaling is activated normally upon EGF stimulation (Inoki et al., 2003). Therefore, I propose that the observed decrease in protein synthesis upon LYCAT silencing is due to a decrease in phosphorylation of TSC2.

In Figure 3.5.2, I showed that two methods of LYCAT gene silencing led to an impairment of cell growth and a reduction in overall cell abundance, when compared to control. In MDA-MB-231 cells transfected with siRNA targeting LYCAT, I observed a decrease in phase confluence over 72 h, along with an increase in CellTox green object count (Figure 3.5.2A-C). CellTox green is a dye that is excluded from viable cells but preferentially stains DNA from apoptotic cells, allowing us to measure cell death. In MDA-MB-231 CRISPR Cas9 cells engineered to stably knockdown LYCAT expression, I observed a decrease in relative cell confluence compared to control (Figure 3.5.2D-F). As previously described, upon LYCAT silencing I observed a decrease in the phosphorylation of GSK3ß. GSK3 is a serine/threonine protein kinase which is able to

phosphorylate a number of downstream targets. GSK3-mediated phosphorylation of cyclins, c-*jun* and c-*myc,* labels them for proteasomal degradation (Duda et al., 2020). Specifically, c-*myc* is a transcription factor that regulates the expression of many target genes that coordinate cell growth and proliferation. When GSK3ß is phosphorylated by Akt, this results in the negative regulation of GSK3ß activity. Further, this phosphorylation leads to enhanced c-*jun* and c-*myc* stability, promoting cell proliferation (Melnik et al., 2019). It has been shown that the nuclear localization of GSK3ß is regulated by mTORC1 activity. Impaired mTORC1 activity results in the translocation of GSK3ß to the nucleus where it is able to degrade c-*myc* (Bautista et al., 2018). Upon LYCAT silencing, we observed a decrease in GSK3ß phosphorylation. This decrease in GSK3ß phosphorylation leads to degradation of c-*myc* and impaired cell growth. Thus, I predict that the effect seen on proliferation and apoptosis is due, in part, to the reduction in phosphorylated GSK3ß and impaired mTORC1 activity, upon LYCAT silencing.

Our groups have previously shown that LYCAT is involved in regulating PIP localization and acyl chain composition (Bone et al., 2017). Specifically, LYCAT silencing causes impaired $PI(4,5)P_2$ synthesis and turnover. Since $PI(4,5)P_2$ is an important precursor for $PI(3,4,5)P_3$, we hypothesized that LYCAT would have a role to play in regulating the PI3K-Akt pathway. Therefore, the model that I propose is that LYCAT silencing reduces $PI(4,5)P_2$ and $PI(3,4,5)P_3$ levels, resulting in less recruitment and activation of PI3K and Akt. Additionally, I predict that PI3K preferentially binds to $PI(4,5)P_2$ with specific acyl chain profiles. The change in acyl chain profile induced by LYCAT silencing will also impair PI3K activity and subsequent Akt phosphorylation. Less Akt activation will result in a reduction in the phosphorylation of substrates downstream of Akt such as TSC2

and GSK3ß. Since the phosphorylation of these substrates are reduced, protein synthesis and cell proliferation will also be impaired.

CHAPTER 5: CONCLUSIONS AND FUTURE DIRECTIONS

In conclusion, my work presents evidence that the acyltransferase LYCAT has a role to play in regulating the PI3K-Akt pathway and its cellular functions. LYCAT silencing affects the activation of Akt1 and Akt2 in both a wild-type cell line and triple negative breast cancer cell line. This altered activation had effects on select substrates downstream of Akt, including TSC2 and GSK3ß. Moreover, my results suggest that LYCAT is also involved in regulating functional outcomes of the PI3K-Akt pathway. While we hypothesize that the reduction in Akt phosphorylation is due to less $PI(3,4,5)P_3$, we are unsure of whether this is also due to an effect on PI3K activity. Further studies should seek to test whether the binding of PI3K to $PI(3,4,5)P_3$ is affected. Additionally, we should examine whether LYCAT silencing has an effect on the recruitment and activation of adaptor proteins, Grb2 and Gab1.

We observed a decrease in puromycylated nascent peptides upon LYCAT silencing, indicating a disruption in protein synthesis and mRNA translation. To further elucidate the mechanism by which LYCAT regulates protein synthesis, insight into the phosphorylation of mTOR, S6K and 4E-BP1 would be beneficial for future work. We also observed a decrease in cell proliferation and an increase in apoptosis, upon LYCAT perturbation. Since the regulation of proliferation and cell survival is complex, further studies should look beyond the PI3K-Akt pathway. The MAPK/ERK pathway is responsible for transmitting signals that result in the prevention or induction of apoptosis and cell cycle progression (Chang et al., 2003). Further studies should seek to explore whether LYCAT affects MAPK/ERK signaling. This could potentially provide insight into how LYCAT regulates these key cellular outcomes. Additionally, future work

should seek to understand what other aspects of the PI3K-Akt pathway are affected, such as metabolism and migration. We could use the Incucyte SX5 to perform ATP assays to gain understanding in how LYCAT silencing promotes certain metabolic changes. Since $PI(4,5)P_2$ and $PI(3,4,5)P_3$ are important for regulating the actin cytoskeleton, it will be important to investigate the effect of LYCAT silencing on migration and invasion. Studies should focus on examining the organization of the actin cytoskeleton, changes in actin machinery, and activity of Rho-family GTPases.

In addition to PIPs, LYCAT has also been shown to alter the acyl chain profile of cardiolipin (Cao et al., 2004; Huang et al., 2014; Zhao et al., 2009). Cardiolipin is an important phospholipid that is highly enriched in the mitochondria and contributes up to 20% of total lipids (Gebert et al., 2009; Schlame & Greenberg, 2017; Tatsuta & Langer, 2017). As it predominantly presents in mitochondria, cardiolipin plays critical roles in many mitochondrial processes including maintaining membrane potential and fluidity, respiration and energy conversion. One study found that LYCAT regulates non-small-cell lung cancer (NSCLC) cell proliferation and migration by modulating mitochondrial dynamics (Huang et al., 2020). Future work should aim to elucidate the effects of LYCAT silencing on mitochondrial dynamics in ARPE-19 and MDA-MB-231 cells.

Upon investigating the effect of LYCAT silencing on EGFR signaling, we observed cell specific differences. Total EGFR levels in ARPE-19 cells remain the same across conditions, while a slight increase in activation was observed in LYCAT silenced cells. On the other hand, while total levels in MDA-MB-231 cells also remained constant, there was a decrease in EGFR

phosphorylation upon LYCAT silencing. This suggests that cell specific differences exist and that MDA-MB-231 cells potentially suffer a double hit in terms of a decrease in $PI(4,5)P_2$ levels as well as a decrease in EGFR activation. Our lab previously found that LYCAT silencing does not alter EGFR cell surface levels or activation in ARPE-19 cells. It will be important to measure cell surface EGFR levels to further solidify our understanding of how LYCAT affects EGFR signalling in MDA-MB-231 cells.

Throughout my research, I used two different cell lines. Specifically, MDA-MB-231 cells are a triple negative breast cancer cell line with no known mutations in PI3K. It would be interesting to investigate the effect of LYCAT silencing in cell lines with mutations that affect PI3K-Akt signaling. Further studies should utilize cells such as SUM149 PT, which display elevated constitutive Akt signaling as a result of PTEN mutation, or MDA-MB-361 cells which have mutations in PI3KCA. Including these cell lines in our studies will help us to further understand how LYCAT affects PI3K-Akt signaling. Additionally, my work validated an alternative model for LYCAT gene silencing. This CRISPR/Cas9 system proved to be efficient in inducing a robust decrease in LYCAT levels and phospho-Akt levels. This model will be useful for future studies and experiments that require stable LYCAT silencing. Further experiments should be done to test the validity of this model in regulating key Akt substrates.

Ultimately, my work provides insight into how LYCAT controls components of the PI3K-Akt pathway and the key cellular functions they regulate. Comparing two cell lines, a non-transformed cell, ARPE-19, and triple negative breast cancer cells, MDA-MB-231, this study

provides evidence for cell specific differences. Our results prove that LYCAT impairs aspects of cell growth and proliferation which may provide a basis for understanding how LYCAT may be targeted for certain therapeutics.

REFERENCES

Abraham, A. G., & O'Neill, E. (2014). PI3K/Akt-mediated regulation of p53 in cancer. *Biochemical Society Transactions*, *42*(4), 798–803. https://doi.org/10.1042/BST20140070

Achiriloaie, M., Barylko, B., & Albanesi, J. P. (1999). Essential Role of the Dynamin Pleckstrin Homology Domain in Receptor-Mediated Endocytosis. *Molecular and Cellular Biology*, *19*(2), 1410–1415. https://doi.org/10.1128/mcb.19.2.1410

Aloulou, A., Ali, Y. Ben, Bezzine, S., Gargouri, Y., & Gelb, M. H. (2012). Phospholipases: An overview. In *Methods in Molecular Biology* (Vol. 861, pp. 63–85). Methods Mol Biol. https://doi.org/10.1007/978-1-61779-600-5_4

Antonescu, C. N., Danuser, G., & Schmid, S. L. (2010). Phosphatidic acid plays a regulatory role in clathrin-mediated endocytosis. *Molecular Biology of the Cell*, *21*(16), 2944–2952. https://doi.org/10.1091/MBC.E10-05-0421/ASSET/IMAGES/LARGE/ZMK0161095450007.JPEG

Audhya, A., Foti, M., & Emr, S. D. (2000). Distinct roles for the yeast phosphatidylinositol 4-Kinases, Stt4p and Pik1p, in secretion, cell growth, and organelle membrane dynamics. *Molecular Biology of the Cell*, *11*(8), 2673–2689. https://doi.org/10.1091/mbc.11.8.2673

Auger, K. R., Serunian, L. A., Soltoff, S. P., Libby, P., & Cantley, L. C. (1989). PDGF-dependent tyrosine phosphorylation stimulates production of novel polyphosphoinositides in intact cells. *Cell*, *57*(1), 167–175. https://doi.org/10.1016/0092-8674(89)90182-7

Balla, T. (2013). Phosphoinositides: Tiny lipids with giant impact on cell regulation. In *Physiological Reviews* (Vol. 93, Issue 3, pp. 1019–1137). American Physiological Society Bethesda, MD. https://doi.org/10.1152/physrev.00028.2012

Balsinde, J., Balboa, M. A., & Dennis, E. A. (1997). Antisense inhibition of group VI Ca2+-independent phospholipase A2 blocks phospholipid fatty acid remodeling in murine P388D1 macrophages. *Journal of Biological Chemistry*, *272*(46), 29317–29321. https://doi.org/10.1074/jbc.272.46.29317

Bautista, S. J., Boras, I., Vissa, A., Mecica, N., Yip, C. M., Kim, P. K., & Antonescu, C. N. (2018). mTOR complex 1 controls the nuclear localization and function of glycogen synthase kinase 3β. *Journal of Biological Chemistry*, *293*(38), 14723–14739.

https://doi.org/10.1074/JBC.RA118.002800/ATTACHMENT/FEE131C3-BEF0-49B9-8647-367D60652CB4/MMC1.PDF

Bone, L. N., Dayam, R. M., Lee, M., Kono, N., Fairn, G. D., Arai, H., Botelho, R. J., & Antonescu, C. N. (2017). The acyltransferase LYCAT controls specific phosphoinositides and related membrane traffic. *Molecular Biology of the Cell*, *28*(1), 161–172. https://doi.org/10.1091/mbc.E16-09-0668

Bozelli, J. C., & Epand, R. M. (2019). Specificity of Acyl Chain Composition of Phosphatidylinositols. *PROTEOMICS*. https://doi.org/10.1002/pmic.201900138

Burke, J. E., & Williams, R. L. (2015). Synergy in activating class I PI3Ks. *Trends in Biochemical Sciences*, *40*(2), 88–100. https://doi.org/10.1016/J.TIBS.2014.12.003

Cabral-Dias, R., Lucarelli, S., Zak, K., Rahmani, S., Judge, G., Abousawan, J., DiGiovanni, L. F., Vural, D., Anderson, K. E., Sugiyama, M. G., Genc, G., Hong, W., Botelho, R. J., Fairn, G. D., Kim, P. K., & Antonescu, C. N. (2022). Fyn and TOM1L1 are recruited to clathrin-coated pits and regulate Akt signaling. *The Journal of Cell Biology*, *221*(4). https://doi.org/10.1083/JCB.201808181/213045

Cao, J., Liu, Y., Lockwood, J., Burn, P., & Shi, Y. (2004a). A novel cardiolipin-remodeling pathway revealed by a gene encoding an endoplasmic reticulum-associated acyl-CoA:lysocardiolipin acyltransferase (ALCAT1) in mouse. *Journal of Biological Chemistry*, *279*(30), 31727–31734. https://doi.org/10.1074/jbc.M402930200

Cao, J., Liu, Y., Lockwood, J., Burn, P., & Shi, Y. (2004b). A Novel Cardiolipin-remodeling Pathway Revealed by a Gene Encoding an Endoplasmic Reticulum-associated Acyl-CoA:Lysocardiolipin Acyltransferase (ALCAT1) in Mouse *. *Journal of Biological Chemistry*, *279*(30), 31727–31734. https://doi.org/10.1074/JBC.M402930200

Cao, J., Shen, W., Chang, Z., & Shi, Y. (2009). ALCAT1 is a polyglycerophospholipid acyltransferase potently regulated by adenine nucleotide and thyroid status. *American Journal of Physiology-Endocrinology and Metabolism*, *296*(4), E647–E653. https://doi.org/10.1152/ajpendo.90761.2008

Chang, F., Steelman, L. S., Lee, J. T., Shelton, J. G., Navolanic, P. M., Blalock, W. L., Franklin, R. A., & McCubrey, J. A. (2003). Signal transduction mediated by the Ras/Raf/MEK/ERK pathway

from cytokine receptors to transcription factors: Potential targeting for therapeutic intervention. *Leukemia*, *17*(7), 1263–1293. https://doi.org/10.1038/SJ.LEU.2402945

Chibaya, L., Karim, B., Zhang, H., & Jones, S. N. (2021). Mdm2 phosphorylation by Akt regulates the p53 response to oxidative stress to promote cell proliferation and tumorigenesis. *Proceedings of the National Academy of Sciences of the United States of America*, *118*(4). https://doi.org/10.1073/PNAS.2003193118/SUPPL_FILE/PNAS.2003193118.SAPP.PDF

Cho, H., Mu, J., Kim, J. K., Thorvaldsen, J. L., Chu, Q., Crenshaw, E. B., Kaestner, K. H., Bartolomei, M. S., Shulman, G. I., & Birnbaum, M. J. (2001). Insulin resistance and a diabetes mellitus-like syndrome in mice lacking the protein kinase Akt2 (PKBβ). *Science*, *292*(5522), 1728–1731. https://doi.org/10.1126/SCIENCE.292.5522.1728

Choo, A. Y., Yoon, S. O., Sang, G. K., Roux, P. P., & Blenis, J. (2008). Rapamycin differentially inhibits S6Ks and 4E-BP1 to mediate cell-type-specific repression of mRNA translation. *Proceedings of the National Academy of Sciences of the United States of America*, *105*(45), 17414–17419. https://doi.org/10.1073/PNAS.0809136105/SUPPL_FILE/0809136105SI.PDF

Choy, C. H., Han, B. K., & Botelho, R. J. (2017). Phosphoinositide Diversity, Distribution, and Effector Function: Stepping Out of the Box. In *BioEssays*. https://doi.org/10.1002/bies.201700121

Cullen, P. J., Cozier, G. E., Banting, G., & Mellor, H. (2001). Modular phosphoinositide-binding domains - Their role in signalling and membrane trafficking. In *Current Biology* (Vol. 11, Issue 21). Cell Press. https://doi.org/10.1016/S0960-9822(01)00523-1

Di Paolo, G., & De Camilli, P. (2006). Phosphoinositides in cell regulation and membrane dynamics. In *Nature* (Vol. 443, Issue 7112, pp. 651–657). Nature Publishing Group. https://doi.org/10.1038/nature05185

Díaz, M. E., González, L., Miquet, J. G., Martínez, C. S., Sotelo, A. I., Bartke, A., & Turyn, D. (2012). Growth hormone modulation of EGF-induced PI3K-Akt pathway in mice liver. *Cellular Signalling*, *24*(2), 514. https://doi.org/10.1016/J.CELLSIG.2011.10.001

D'Souza, K., & Epand, R. M. (2014). Enrichment of phosphatidylinositols with specific acyl chains. *Biochimica et Biophysica Acta - Biomembranes*, *1838*(6), 1501–1508. https://doi.org/10.1016/j.bbamem.2013.10.003

Du, Z., & Lovly, C. M. (2018). Mechanisms of receptor tyrosine kinase activation in cancer. *Molecular Cancer 2018 17:1*, *17*(1), 1–13. https://doi.org/10.1186/S12943-018-0782-4

Duda, P., Akula, S. M., Abrams, S. L., Steelman, L. S., Martelli, A. M., Cocco, L., Ratti, S., Candido, S., Libra, M., Montalto, G., Cervello, M., Gizak, A., Rakus, D., & McCubrey, J. A. (2020). Targeting GSK3 and Associated Signaling Pathways Involved in Cancer. *Cells*, *9*(5), 1110. https://doi.org/10.3390/cells9051110

Engelman, J. A., Luo, J., & Cantley, L. C. (2006). The evolution of phosphatidylinositol 3-kinases as regulators of growth and metabolism. *Nature Reviews Genetics 2006 7:8*, *7*(8), 606–619. https://doi.org/10.1038/nrg1879

Falkenburger, B. H., Jensen, J. B., Dickson, E. J., Suh, B. C., & Hille, B. (2010). Phosphoinositides: Lipid regulators of membrane proteins. *Journal of Physiology*, *588*(17), 3179–3185. https://doi.org/10.1113/jphysiol.2010.192153

Feng, J., Tamaskovic, R., Yang, Z., Brazil, D. P., Merlo, A., Hess, D., & Hemmings, B. A. (2004). Stabilization of Mdm2 via decreased ubiquitination is mediated by protein kinase B/Akt-dependent phosphorylation. *The Journal of Biological Chemistry*, *279*(34), 35510–35517. https://doi.org/10.1074/JBC.M404936200

Garcia, P., Gupta, R., Shah, S., Morris, A. J., Rudge, S. A., Scarlata, S., Petrova, V., McLaughlin, S., & Rebecchi, M. J. (1995). The pleckstrin homology domain of phospholipase C-delta 1 binds with high affinity to phosphatidylinositol 4,5-bisphosphate in bilayer membranes. *Biochemistry*, *34*(49), 16228–16234. https://doi.org/10.1021/BI00049A039

Gebert, N., Joshi, A. S., Kutik, S., Becker, T., McKenzie, M., Guan, X. L., Mooga, V. P., Stroud, D. A., Kulkarni, G., Wenk, M. R., Rehling, P., Meisinger, C., Ryan, M. T., Wiedemann, N., Greenberg, M. L., & Pfanner, N. (2009). Mitochondrial Cardiolipin Involved in Outer-Membrane Protein Biogenesis: Implications for Barth Syndrome. *Current Biology*, *19*(24), 2133–2139. https://doi.org/10.1016/j.cub.2009.10.074

Goh, L. K., & Sorkin, A. (2013). Endocytosis of Receptor Tyrosine Kinases. *Cold Spring Harbor Perspectives in Biology*, *5*(5), a017459. https://doi.org/10.1101/CSHPERSPECT.A017459

Hammond, G. R. V., & Balla, T. (2015). Polyphosphoinositide binding domains: Key to inositol lipid biology. In *Biochimica et Biophysica Acta - Molecular and Cell Biology of Lipids* (Vol. 1851, Issue 6, pp. 746–758). Elsevier B.V. https://doi.org/10.1016/j.bbalip.2015.02.013

Hemmings, B. A., & Restuccia, D. F. (2012). PI3K-PKB/Akt pathway. *Cold Spring Harbor Perspectives in Biology*, *4*(9). https://doi.org/10.1101/cshperspect.a011189

Hers, I., Vincent, E. E., & Tavaré, J. M. (2011). Akt signalling in health and disease. *Cellular Signalling*, *23*(10), 1515–1527. https://doi.org/10.1016/J.CELLSIG.2011.05.004

Hicks, A. M., DeLong, C. J., Thomas, M. J., Samuel, M., & Cui, Z. (2006). Unique molecular signatures of glycerophospholipid species in different rat tissues analyzed by tandem mass spectrometry. *Biochimica et Biophysica Acta - Molecular and Cell Biology of Lipids*, *1761*(9), 1022–1029. https://doi.org/10.1016/j.bbalip.2006.05.010

Huang, L. S., Kotha, S. R., Avasarala, S., VanScoyk, M., Winn, R. A., Pennathur, A., Yashaswini, P. S., Bandela, M., Salgia, R., Tyurina, Y. Y., Kagan, V. E., Zhu, X., Reddy, S. P., Sudhadevi, T., Punathil-Kannan, P. K., Harijith, A., Ramchandran, R., Bikkavilli, R. K., & Natarajan, V. (2020). Lysocardiolipin acyltransferase regulates NSCLC cell proliferation and migration by modulating mitochondrial dynamics. *The Journal of Biological Chemistry*, *295*(38), 13393–13406. https://doi.org/10.1074/JBC.RA120.012680

Huang, L. S., Mathew, B., Li, H., Zhao, Y., Ma, S. F., Noth, I., Reddy, S. P., Harijith, A., Usatyuk, P. V., Berdyshev, E. V., Kaminski, N., Zhou, T., Zhang, W., Zhang, Y., Rehman, J., Kotha, S. R., Gurney, T. O., Parinandi, N. L., Lussier, Y. A., … Natarajan, V. (2014). The mitochondrial cardiolipin remodeling enzyme lysocardiolipin acyltransferase is a novel target in pulmonary fibrosis. *American Journal of Respiratory and Critical Care Medicine*, *189*(11), 1402–1415. https://doi.org/10.1164/rccm.201310-1917OC

Hubbard, S. R., & Miller, W. T. (2007). Receptor tyrosine kinases: mechanisms of activation and signaling. *Current Opinion in Cell Biology*, *19*(2), 117–123. https://doi.org/10.1016/J.CEB.2007.02.010

Imae, R., Inoue, T., Nakasaki, Y., Uchida, Y., Ohba, Y., Kono, N., Nakanishi, H., Sasaki, T., Mitani, S., & Arai, H. (2012). LYCAT, a homologue of C. elegans acl-8, acl-9, and acl-10, determines

the fatty acid composition of phosphatidylinositol in mice. *Journal of Lipid Research*, *53*(3), 335–347. https://doi.org/10.1194/jlr.M018655

Inoki, K., Li, Y., Xu, T., & Guan, K. L. (2003). Rheb GTPase is a direct target of TSC2 GAP activity and regulates mTOR signaling. *Genes & Development*, *17*(15), 1829–1834. https://doi.org/10.1101/GAD.1110003

Inoue, A., & Aoki, J. (2017). *Future Lipidology Phospholipase A 1 : structure, distribution and function*. https://doi.org/10.2217/17460875.1.6.687

Jeschke, A., Zehethofer, N., Lindner, B., Krupp, J., Schwudke, D., Haneburger, I., Jovic, M., Backer, J. M., Balla, T., Hilbi, H., & Haas, A. (2015). Phosphatidylinositol 4-phosphate and phosphatidylinositol 3-phosphate regulate phagolysosome biogenesis. *Proceedings of the National Academy of Sciences of the United States of America*, *112*(15), 4636–4641. https://doi.org/10.1073/pnas.1423456112

Jethwa, N., Chung, G. H. C., Lete, M. G., Alonso, A., Byrne, R. D., Calleja, V., & Larijani, B. (2015). Endomembrane PtdIns(3,4,5)P3 activates the PI3K-Akt pathway. *Journal of Cell Science*, *128*(18), 3456–3465. https://doi.org/10.1242/jcs.172775

Kim, Y. J., Guzman-Hernandez, M. L., & Balla, T. (2011). A highly dynamic ER-derived phosphatidylinositol-synthesizing organelle supplies phosphoinositides to cellular membranes. *Developmental Cell*, *21*(5), 813–824. https://doi.org/10.1016/j.devcel.2011.09.005

Laux, T., Fukami, K., Thelen, M., Golub, T., Frey, D., & Caroni, P. (2000). GAP43, MARCKS, and CAP23 modulate PI(4,5)P(2) at plasmalemmal rafts, and regulate cell cortex actin dynamics through a common mechanism. *The Journal of Cell Biology*, *149*(7), 1455–1471. https://doi.org/10.1083/JCB.149.7.1455

Lemmon, M. A., & Ferguson, K. M. (2000). Signal-dependent membrane targeting by pleckstrin homology (PH) domains. In *Biochemical Journal* (Vol. 350, Issue 1, pp. 1–18). https://doi.org/10.1042/0264-6021:3500001

Leung, D. W. (2001). The structure and functions of human lysophosphatidic acid acyltransferases. In *Frontiers in bioscience : a journal and virtual library* (Vol. 6). Front Biosci. https://doi.org/10.2741/leung

Li, J., Liu, X., Wang, H., Zhang, W., Chan, D. C., & Shi, Y. (2012). Lysocardiolipin acyltransferase 1 (ALCAT1) controls mitochondrial DNA fidelity and biogenesis through modulation of MFN2 expression. *Proceedings of the National Academy of Sciences of the United States of America*, *109*(18), 6975–6980. https://doi.org/10.1073/pnas.1120043109

Li, J., Romestaing, C., Han, X., Li, Y., Hao, X., Wu, Y., Sun, C., Liu, X., Jefferson, L. S., Xiong, J., Lanoue, K. F., Chang, Z., Lynch, C. J., Wang, H., & Shi, Y. (2010). Cardiolipin remodeling by ALCAT1 links oxidative stress and mitochondrial dysfunction to obesity. *Cell Metabolism*, *12*(2), 154–165. https://doi.org/10.1016/j.cmet.2010.07.003

Li, Y., Corradetti, M. N., Inoki, K., & Guan, K. L. (2004). TSC2: filling the GAP in the mTOR signaling pathway. *Trends in Biochemical Sciences*, *29*(1), 32–38. https://doi.org/10.1016/J.TIBS.2003.11.007

Lien, E. C., Dibble, C. C., & Toker, A. (2017). PI3K signaling in cancer: beyond AKT. In *Current Opinion in Cell Biology* (Vol. 45, pp. 62–71). Elsevier Ltd. https://doi.org/10.1016/j.ceb.2017.02.007

Liu, S. L., Wang, Z. G., Hu, Y., Xin, Y., Singaram, I., Gorai, S., Zhou, X., Shim, Y., Min, J. H., Gong, L. W., Hay, N., Zhang, J., & Cho, W. (2018). Quantitative Lipid Imaging Reveals a New Signaling Function of Phosphatidylinositol-3,4-Bisphophate: Isoform- and Site-Specific Activation of Akt. *Molecular Cell*, *71*(6), 1092-1104.e5. https://doi.org/10.1016/j.molcel.2018.07.035

Lopez-Pajares, V., Kim, M. M., & Yuan, Z. M. (2008). Phosphorylation of MDMX Mediated by Akt Leads to Stabilization and Induces 14-3-3 Binding. *The Journal of Biological Chemistry*, *283*(20), 13707. https://doi.org/10.1074/JBC.M710030200

Manning, B. D., & Cantley, L. C. (2007). AKT/PKB Signaling: Navigating Downstream. In *Cell* (Vol. 129, Issue 7, pp. 1261–1274). Elsevier. https://doi.org/10.1016/j.cell.2007.06.009

Manning, B. D., & Toker, A. (2017). AKT/PKB Signaling: Navigating the Network. In *Cell* (Vol. 169, Issue 3, pp. 381–405). Cell Press. https://doi.org/10.1016/j.cell.2017.04.001

Matheny, R. W., & Adamo, M. L. (2009). Current Perspectives on Akt Akt-ivation and Akt-ions: *Https://Doi.Org/10.3181/0904-MR-138*, *234*(11), 1264–1270. https://doi.org/10.3181/0904-MR-138

Mayinger, P. (2012). Phosphoinositides and vesicular membrane traffic. In *Biochimica et Biophysica Acta - Molecular and Cell Biology of Lipids* (Vol. 1821, Issue 8, pp. 1104–1113). NIH Public Access. https://doi.org/10.1016/j.bbalip.2012.01.002

Mayo, L. D., & Donner, D. B. (2001). A phosphatidylinositol 3-kinase/Akt pathway promotes translocation of Mdm2 from the cytoplasm to the nucleus. *Proceedings of the National Academy of Sciences of the United States of America*, *98*(20), 11598–11603. https://doi.org/10.1073/PNAS.181181198/ASSET/F5698EB4-E515-4424-AFF8-2C938CC5FE8A/ASSETS/GRAPHIC/PQ1811811004.JPEG

Melnik, S., Werth, N., Boeuf, S., Hahn, E. M., Gotterbarm, T., Anton, M., & Richter, W. (2019). Impact of c-MYC expression on proliferation, differentiation, and risk of neoplastic transformation of human mesenchymal stromal cells. *Stem Cell Research and Therapy*, *10*(1), 1–18. https://doi.org/10.1186/S13287-019-1187-Z/FIGURES/6

Milne, S. B., Ivanova, P. T., DeCamp, D., Hsueh, R. C., & Brown, H. A. (2005). A targeted mass spectrometric analysis of phosphatidylinositol phosphate species. *Journal of Lipid Research*, *46*(8), 1796–1802. https://doi.org/10.1194/jlr.D500010-JLR200

Mücksch, F., Citir, M., Lüchtenborg, C., Glass, B., Traynor-Kaplan, A., Schultz, C., Brügger, B., & Kräusslich, H. G. (2019). Quantification of phosphoinositides reveals strong enrichment of PIP2 in HIV-1 compared to producer cell membranes. *Scientific Reports 2019 9:1*, *9*(1), 1–13. https://doi.org/10.1038/s41598-019-53939-z

Mutch, L. J., Howden, J. D., Jenner, E. P. L., Poulter, N. S., & Rappoport, J. Z. (2014). Polarised Clathrin-Mediated Endocytosis of EGFR During Chemotactic Invasion. *Traffic*, *15*(6), 648–664. https://doi.org/10.1111/TRA.12165

Nakatsu, F., Perera, R. M., Lucast, L., Zoncu, R., Domin, J., Gertler, F. B., Toomre, D., & de Camilli, P. (2010). The inositol 5-phosphatase SHIP2 regulates endocytic clathrin-coated pit dynamics. *Journal of Cell Biology*, *190*(3), 307–315. https://doi.org/10.1083/JCB.201005018/VIDEO-4

Rieusset, J. (2018). The role of endoplasmic reticulum-mitochondria contact sites in the control of glucose homeostasis: An update. *Cell Death and Disease*, *9*(3), 1–12. https://doi.org/10.1038/s41419-018-0416-1

Rosen, S. A. J., Gaffney, P. R. J., Spiess, B., & Gould, I. R. (2012). Understanding the relative affinity and specificity of the pleckstrin homology domain of protein kinase B for inositol phosphates. *Physical Chemistry Chemical Physics*, *14*(2), 929–936. https://doi.org/10.1039/c1cp22240f

Sasaki, T., Takasuga, S., Sasaki, J., Kofuji, S., Eguchi, S., Yamazaki, M., & Suzuki, A. (2009). Mammalian phosphoinositide kinases and phosphatases. In *Progress in Lipid Research* (Vol. 48, Issue 6, pp. 307–343). Pergamon. https://doi.org/10.1016/j.plipres.2009.06.001

Saxton, R. A., & Sabatini, D. M. (2017). mTOR Signaling in Growth, Metabolism, and Disease. In *Cell* (Vol. 168, Issue 6, pp. 960–976). Cell Press. https://doi.org/10.1016/j.cell.2017.02.004

Schlame, M., & Greenberg, M. L. (2017). Biosynthesis, remodeling and turnover of mitochondrial cardiolipin. In *Biochimica et Biophysica Acta - Molecular and Cell Biology of Lipids* (Vol. 1862, Issue 1, pp. 3–7). Elsevier B.V. https://doi.org/10.1016/j.bbalip.2016.08.010

Schmid, A. C., Wise, H. M., Mitchell, C. A., Nussbaum, R., & Woscholski, R. (2004). Type II phosphoinositide 5-phosphatases have unique sensitivities towards fatty acid composition and head group phosphorylation. *FEBS Letters*, *576*(1–2), 9–13. https://doi.org/10.1016/j.febslet.2004.08.052

Shindou, H., Eto, M., Morimoto, R., & Shimizu, T. (2009). Identification of membrane O-acyltransferase family motifs. *Biochemical and Biophysical Research Communications*, *383*(3), 320–325. https://doi.org/10.1016/j.bbrc.2009.04.013

Shindou, H., Hishikawa, D., Harayama, T., Eto, M., & Shimizu, T. (2017). Generation of membrane diversity by lysophospholipid acyltransferases. *J. Biochem*, *154*(1), 21–28. https://doi.org/10.1093/jb/mvt048

Shiojima, I., Sato, K., Izumiya, Y., Schiekofer, S., Ito, M., Liao, R., Colucci, W. S., & Walsh, K. (2005). Disruption of coordinated cardiac hypertrophy and angiogenesis contributes to the transition to heart failure. *The Journal of Clinical Investigation*, *115*. https://doi.org/10.1172/JCI24682

Shulga, Y. V., Anderson, R. A., Topham, M. K., & Epand, R. M. (2012). Phosphatidylinositol-4-phosphate 5-kinase isoforms exhibit acyl chain selectivity for both substrate and lipid

activator. *Journal of Biological Chemistry*, *287*(43), 35953–35963. https://doi.org/10.1074/jbc.M112.370155

Sigismund, S., Argenzio, E., Tosoni, D., Cavallaro, E., Polo, S., & di Fiore, P. P. (2008). Clathrin-Mediated Internalization Is Essential for Sustained EGFR Signaling but Dispensable for Degradation. *Developmental Cell*, *15*(2), 209–219. https://doi.org/10.1016/J.DEVCEL.2008.06.012

Soltoff, S. P., Kaplan, D. R., & Cantley, L. C. (1993). Phosphatidylinositol 3-Kinase. *Methods in Neurosciences*, *18*(C), 100–112. https://doi.org/10.1016/B978-0-12-185285-6.50018-X

Stad, R., Ramos, Y. F. M., Little, N., Grivell, S., Attema, J., van der Eb, A. J., & Jochemsen, A. G. (2000). Hdmx Stabilizes Mdm2 and p53 *. *Journal of Biological Chemistry*, *275*(36), 28039–28044. https://doi.org/10.1074/JBC.M003496200

Takeuchi, K., & Reue, K. (2009). Biochemistry, physiology, and genetics of GPAT, AGPAT, and lipin enzymes in triglyceride synthesis. In *American Journal of Physiology - Endocrinology and Metabolism* (Vol. 296, Issue 6, pp. 1195–1209). American Physiological Society. https://doi.org/10.1152/ajpendo.90958.2008

Tatsuta, T., & Langer, T. (2017). Intramitochondrial phospholipid trafficking. In *Biochimica et Biophysica Acta - Molecular and Cell Biology of Lipids* (Vol. 1862, Issue 1, pp. 81–89). Elsevier B.V. https://doi.org/10.1016/j.bbalip.2016.08.006

Tomas, A., Futter, C. E., & Eden, E. R. (2014). EGF receptor trafficking: consequences for signaling and cancer. *Trends in Cell Biology*, *24*(1), 26–34. https://doi.org/10.1016/J.TCB.2013.11.002

Tubbesing, K., Ward, J., Abini-Agbomson, R., Malhotra, A., Rudkouskaya, A., Warren, J., Lamar, J., Martino, N., Adam, A. P., & Barroso, M. (2020). Complex Rab4-Mediated Regulation of Endosomal Size and EGFR Activation. *Molecular Cancer Research : MCR*, *18*(5), 757–773. https://doi.org/10.1158/1541-7786.MCR-19-0052/81446/AM/COMPLEX-RAB4-MEDIATED-REGULATION-OF-ENDOSOMAL-SIZE

Van Meer, G., Voelker, D. R., & Feigenson, G. W. (2008). Membrane lipids: Where they are and how they behave. In *Nature Reviews Molecular Cell Biology* (Vol. 9, Issue 2, pp. 112–124). https://doi.org/10.1038/nrm2330

Vanhaesebroeck, B., Leevers, S. J., Panayotou, G., Waterfield, M. D., & Waterfield, M. D. (1997). Phosphoinositide 3-kinases: a conserved family of signal transducers. *Trends in Biochemical Sciences*, *22*(7), 267–272. https://doi.org/10.1016/S0968-0004(97)01061-X

Wallroth, A., & Haucke, V. (2018). Phosphoinositide conversion in endocytosis and the endolysosomal system. In *Journal of Biological Chemistry* (Vol. 293, Issue 5, pp. 1526–1535). American Society for Biochemistry and Molecular Biology Inc. https://doi.org/10.1074/jbc.R117.000629

Wang, W., Ni, L., Yu, Q., Xiong, J., Liu, H. C., & Rosenwaks, Z. (2010). Expression of the Lycat gene in the mouse cardiovascular and female reproductive systems. *Developmental Dynamics*, *239*(6), 1827–1837. https://doi.org/10.1002/dvdy.22300

Watt, S. A., Kular, G., Fleming, I. N., Downes, C. P., & Lucocq, J. M. (2002). Subcellular localization of phosphatidylinositol 4,5-bisphosphate using the pleckstrin homology domain of phospholipase C δ1. *Biochemical Journal*, *363*(3), 657–666. https://doi.org/10.1042/0264-6021:3630657

Yabuuchi, H., & O'Brien, J. S. (1968). Positional distribution of fatty acids in glycerophosphatides of bovine gray matter. *Journal of Lipid Research*, *9*(1), 65–67.

Yang, K., & Han, X. (2016). Lipidomics: Techniques, Applications, and Outcomes Related to Biomedical Sciences. In *Trends in Biochemical Sciences* (Vol. 41, Issue 11, pp. 954–969). Elsevier Ltd. https://doi.org/10.1016/j.tibs.2016.08.010

Yu, Y., Li, S., Xu, X., Li, Y., Guan, K., Arnold, E., & Ding, J. (2005). Structural basis for the unique biological function of small GTPase RHEB. *The Journal of Biological Chemistry*, *280*(17), 17093–17100. https://doi.org/10.1074/JBC.M501253200

Zhao, Y., Chen, Y. Q., Li, S., Konrad, R. J., & Cao, G. (2009). The microsomal cardiolipin remodeling enzyme acyl-CoA lysocardiolipin acyltransferase is an acyltransferase of multiple anionic lysophospholipids. *Journal of Lipid Research*, *50*(5), 945–956. https://doi.org/10.1194/jlr.M800567-JLR200